Blade Optimization of Gravitational Water Vortex Turbine

Thesis submitted in partial fulfillment of the degree of Master of Science in Mechanical Engineering

By

Nauman Hanif Khan

FACULTY OF MECHANICAL ENGINEERING

GHULAM ISHAQ KHAN INSTITUTE OF ENGINEERING SCIENCES AND TECHNOLOGY

May 2016

Blade Optimization of Gravitational Water Vortex Turbine

Thesis submitted in partial fulfillment of the degree of Master of Science in Mechanical Engineering

By

Nauman Hanif Khan

Supervised By

Prof. Dr. Javed Ahmed Chattha

FACULTY OF MECHANICAL ENGINEERING

GHULAM ISHAQ KHAN INSTITUTE OF ENGINEERING SCIENCES AND TECHNOLOGY

May 2016

“Allah is the Light of the heavens and the earth. The parable of His light is, as it were, that of a niche containing a lamp; the lamp is [enclosed] in glass, the glass [shining] like a radiant star: [a lamp] lit from a blessed tree - an olive-tree that is neither of the east nor of the west the oil whereof [is so bright that it] would well-nigh give light [of itself] even though fire had not touched it: light upon light! Allah guides unto His light him that wills [to be guided]; and [to this end] Allah propounds parables unto men, since Allah [alone] has full knowledge of all things.”

AL-NUR, 35

All praise is to ALLAH AL MIGHTY alone.

After that, I dedicate this thesis to my parents for their immense support in every aspect throughout my life. Their love and devotion is what has given me the achievements I have made.

May ALLAH shower HIS unlimited blessings upon us.

DECLARATION OF AUTHOR'S RIGHTS

ACKNOWLEDGEMENTS

The author is deeply thankful to Almighty Allah, the Beneficent the most Merciful, who bestowed him with the strength and courage to complete the study.

The author acknowledges and appreciates the guidance and valuable suggestions of **Prof. Dr. Javed Ahmed Chattha** and **Dr. Taqi Ahmed Cheema** under whose supervision this study has been completed. The author highly acknowledges their cooperation and friendly way of interaction which made the study joyful despite of all the difficulties.

The author is highly thankful to dean of faculty **Dr. S. M. Ahmad** for his immense support, encouragement, suggestions and guidance in all matters, academic or social, throughout the master's studies.

The author is also thankful to **Dr. Khalid Rehman** (Assistant Professor) for his guidance and help in different occasions during the studies which ultimately resulted in increased learning.

The author highly appreciates the help and guidance of **Mr. Muhammad Shakeel** (Graduate Assistant) throughout the tenure of his studies.

THE AUTHOR IS ALSO THANKFUL TO HIS COLLEAGUES AND FRIENDS FOR THEIR SUPPORT AND WHO MADE THE TENURE OF THIS STUDY QUITE LIVELY.

TABLE OF CONTENTS

LIST OF FIGURES:

LIST OF TABLES:

ABSTRACT

Energy generation through water is one of the most economic sources of power. Among the hydro-power plants, micro-hydro power plants are more preferred since they require lower heads and smaller flow rates to generate electricity. The main advantage of micro-hydropower plants is the combination of feasibility, ease of installation, efficiency and economy into a single source of power. In the category of micro-hydro power plants, gravitational water vortex power plants are emerging currently due to their ease of installation, reduced setup time and minimal expertise required for installation.

In this study, a simple methodology has been used to investigate the parameters that result in the formation and strengthening of vortex and an efficient generation of energy using a strong artificial air-core vortex. The analysis of the vortex formation at different basin parameters led to the reduction of the flow-rate in order to increase the efficiency of the plant. Based on different blade shapes, turbine efficiencies were compared at different load conditions using a head of 0.5m. The analysis is carried out using ANSYS CFX, and an experimental setup was fabricated for the validation of the numerical results. The numerical results show great agreement with those obtained experimentally. The proposed methodology can be used to determine the plant specifications and blade size and shape for different flow rates and different heads. This methodology also helps in determination of the approximate power that can be obtained from a specific site.

The maximum plant efficiency of 68.84% was obtained by using cross flow blades which is far better than the efficiency obtained by using other blade profiles for the same discharge and head conditions. This efficiency was verified experimentally with an error in the range of 5 to 12%.

LIST OF NOTATIONS:

ω	Rotational speed of rotor (rad/sec)
γ	Specific weight of water
H	Total Head
Q	Flow rate
T	Torque
N	Rotational speed (rpm)
η	Efficiency
V_r	Radial Velocity, m/s
V_θ	Tangential Velocity, m/s
V_z	Axial Velocity, m/s
H_v	Vortex Height, m
r	Radius, m
g	Gravitational acceleration, m^2/s
α_{air}	Air volume fraction
α_{water}	Water volume fraction
ν	Kinematic viscosity m^2/s
ρ	Density, kg/m^3

CHAPTER 1. INTRODUCTION

The exhaust emissions from fossil fuel operated engines and power plants are a great concern for the modern world, since they are responsible for a number of lungs diseases, infections, and environmental degradation **[1], [2].** Among the available green sources of energy, hydropower has a significant value because of its self-sustainability, economic and environmental benefits **[3], [4].**

1.1 HYDRO-ELECTRIC POWER PLANTS

Hydro-electric power plants can serve as a solution to the current energy crisis of the world since they use the energy stored in a free stream of water to generate electricity rather than using oil and other fuels. In hydro-electric power plants, water is stored at a higher potential. This water is then passed onto the blades of a hydraulic turbine. Using the turbine, mechanical energy can be harnessed from the potential and kinetic energy of the flowing water. Once mechanical energy has been generated, then this energy may be converted to electrical power which can be transmitted through electric lines for use [**5**].

A hydraulic turbine may be classified as impulse and a reaction turbine. In impulse turbines, the rotation of the rotor is caused by the impact of a high velocity jet of fluid on the blades of turbine. The impulse resulting due to the flow of fluid on the blades causes the rotor to rotate. Reaction turbine is the type of turbine, in which the rotor blades rotate as a result of the reaction to the force/weight of the fluid [**5**]. The comparison of reaction and impulse turbines is shown in Figure 1.1.

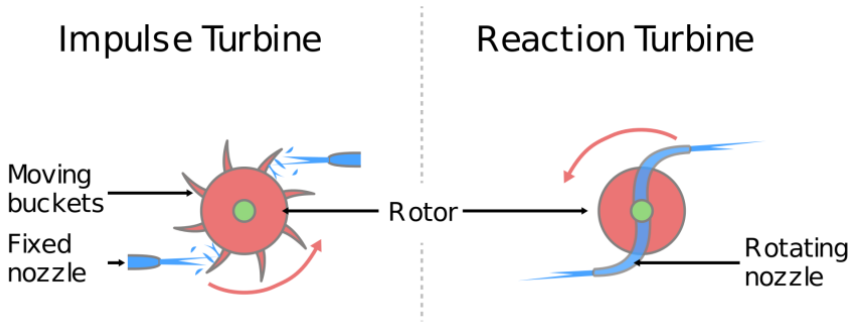

Figure 1. 1 Comparison of Impulse and Reaction Turbines **[6]**

Another classification of the hydraulic turbines may be based upon the pattern of flow. The flow of the fluid in the turbine may either be radial, axial or mixed as shown in Figure 1.3. The turbines may be termed as radial flow, axial flow and mixed

flow turbines respectively. In mixed flow turbines, the flow of the fluid is in radial as well as axial directions.

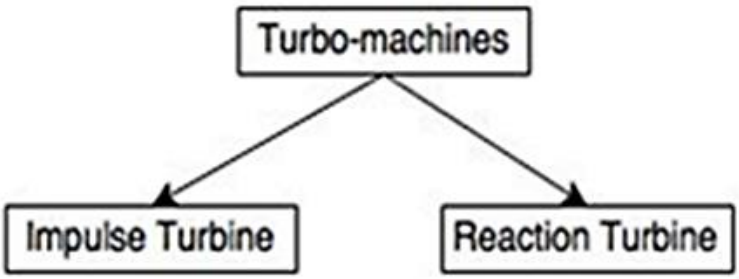

Figure 1. 2 Turbine classification on the basis of working mechanism [5]

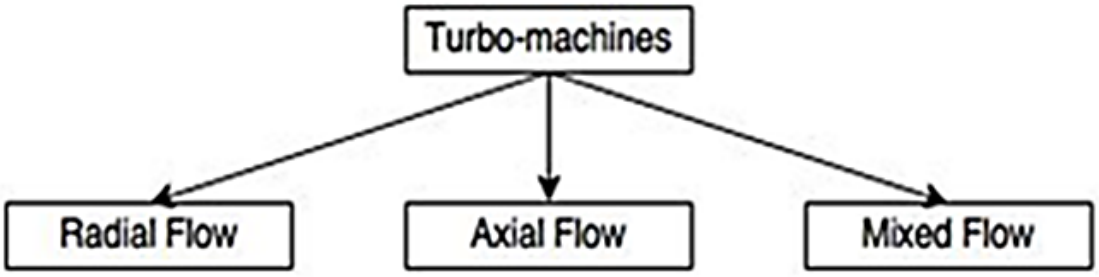

Figure 1. 3 Turbine classification on the basis of flow pattern [5]

Hydro-power plants may also be classified as large, medium, small, mini, micro and pico hydropower plants. This classification is based on the production capacity. [**7**] Besides the main advantage of being environment friendly, hydroelectric power plants have certain advantages over other sources of power generation, which are [**8**]:

i. The running cost of hydro-electric power plants is considerably lesser than thermal power stations since it uses freely available water instead of fuel.
ii. Since there is no fuel usage, therefore the expenditure for fuel purchase, quality check, transportation, storage and ash handling equipment is not incurred in hydro-electric power plants.
iii. It does not produce any hazardous gases and thus does not cause any environmental pollution.
iv. The hydro-electric turbines run at a lower rpm as compared to steam turbines and thus are easy to handle.
v. They are safer as there are no boilers associated with hydro-electric power plants.
vi. The water flowing out of the turbine after the power has been extracted, can be easily used for consumption and irrigation purposes, since it does not contain any harmful pollutants.

vii. Once the initial investment has been recovered, the hydro-electric plants operate almost free of cost.

viii. They do not emit any hazardous radiations as in case of nuclear power plants.

1.2 MICRO-HYDRO POWER PLANTS

Micro-hydro power plants are the types of hydro-electric power plants which are capable of producing a maximum power output of 100kW. They are of smaller size as compared to the conventional hydro-electric power plants and are thus suitable for developing countries, where initial investment is a major issue. Turbines of this type can be installed much more easily since their requirements are not as high as hydro-electric power plants [**7**].

These plants operate on the natural flow of the water (run of the river method) and are capable of providing electrical power to a small nearby community. These plants do not require a dam or huge reservoir for water storage, which reduces the initial investment required for the plant construction. A portion of the water from a river is diverted through a channel, which can be used for the operation of the plant [**9**]. The basic layout out of micro hydro power plant is shown in Figure 1.4.

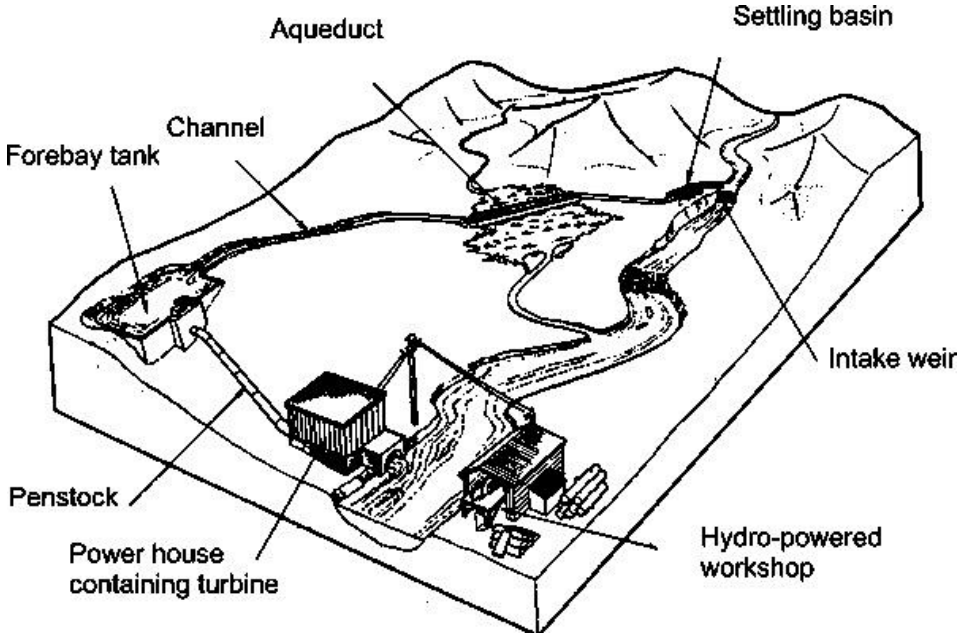

Figure 1. 4 Basic layout out of micro hydro power plant [**10**]

There are various types of micro-hydro turbines [**11**]. Some of these are:

i. Screw Turbine

ii. Turgo Turbine

iii. Split Pipe Turbine
iv. Counter Rotating Turbine
v. Barker's Mill
vi. Cross-flow Turbine
vii. Gravitational Water Vortex Power Plant

Just as hydro power plants have advantages over steam and fuel operated power plants, in the same way, micro-hydro power plants also have certain advantages over other types of power production mechanisms. These advantages are discussed in the following section **[12] [13] [14] [15]:**

i. Micro-hydro power plants require a small flow rate and a small head to generate electric power.
ii. No water storage dams or reservoirs are needed, which reduces the risks associated with dam collapse , thus they can be installed near to the point of utilization.
iii. Since dams and reservoirs are not needed, so this reduces the capital investment required initially.
iv. They operate along the run of river, so they can be installed along the river without disturbing the aquatic life.
v. In regions, which are potentially feasible for hydro-power generation, these can serve as the most cost-effective system due to their free of cost operation and cheaper maintenance.
vi. They have almost no negative impact on the environment.
vii. These power-plants can serve as an off-grid solution to energy crisis and supply electric power to nearby locations.
viii. The cost and losses associated with long transmission lines are minimized in case of micro-hydro power plants, since they are located near to the point of utilization.

1.3 PAKISTAN'S POTENTIAL IN MICRO-HYDRO POWER PLANTS

Fortunately Pakistan has a vast potential for micro hydro power plants, but due to the financial and social problems encountered in the country, this potential has not yet been utilized properly. The enormous potential of Pakistan in micro-hydro Plants is due to the abundant small rivers which are located in the mountaineous and planar

regions of Pakistan. The Hydropower generation potential of Pakistan has been estimated to be approximately 70,000MW which is almost 10 times more than the current hydal power produced [**16**]. This eneromous potential is due to the hilly terrains constituting a large number of rivers and canals. By the proper utilization of these water resources, a lot of energy can be generated. The large number of rivers, canals and waterfalls located in Pakistan, specifically Khyber Pakhtun Khwa (KPK), are a suitable location for the installation of micro-hydro power plants. A large number of micro-hydro power plants have already been installed in Mardan, Chitral, Dir, Mansehra and Shangla [**16**].

1.4 GRAVITATIONAL WATER VORTEX POWER PLANT (GWVPP)

Free surface vortices are a common and an important phenomenon in the field of hydraulic engineering. Vortices are formed at the intake of hydraulic structures due to a design flaw, where a large amount of water is drained into the intake. This flow into the intake causes a vortex to initiate at the free surface due to the Coriolis Force. This vortex gradually intensifies, causes the water rotation to speed up and in turn causes the pressure in the center of the vortex to decrease. This pressure gradually decreases to an extent that ultimately it reduces below the atmospheric pressure and sucks the air into the intake and forms an air core. The radius of the air core gradually reduces while moving from the free surface to the intake [**17**].

The vortex formed may either be in clockwise or anti-clock wise direction, depending upon the location with respect to the equator. In northern hemisphere, the vortex formed is in anticlock-wise direction, while in southern hemosphere, the vortex formed is in clockwise direction [**18**].

The concept of water's natural energy stored in the form of vortex was initially given by Viktor Schauberger (1885-1958) an Austrian forest caretaker and a naturalist, who was commonly known as the water wizard. He observed the circulation of water along a river, when an egg-shaped stone started circling due to the force of the water [**19**].

The idea of Viktor Schauberger was turned into a GWVPP by an Australian engineer, Franz Zotlöterer while trying to aerate water without any external input of power. This was done by generating a vortex in a cylindrical basin with an exit hole at the bottom. The increased surface area of the water would ultimately aerate the water. From the rotational path followed by the water in the air-core vortex, he expected it to

generate rotational energy if a vertical axis rotor was placed at the vortex center [**20**]. The concept of a GWVPP as shown in Figure 1.5 below.

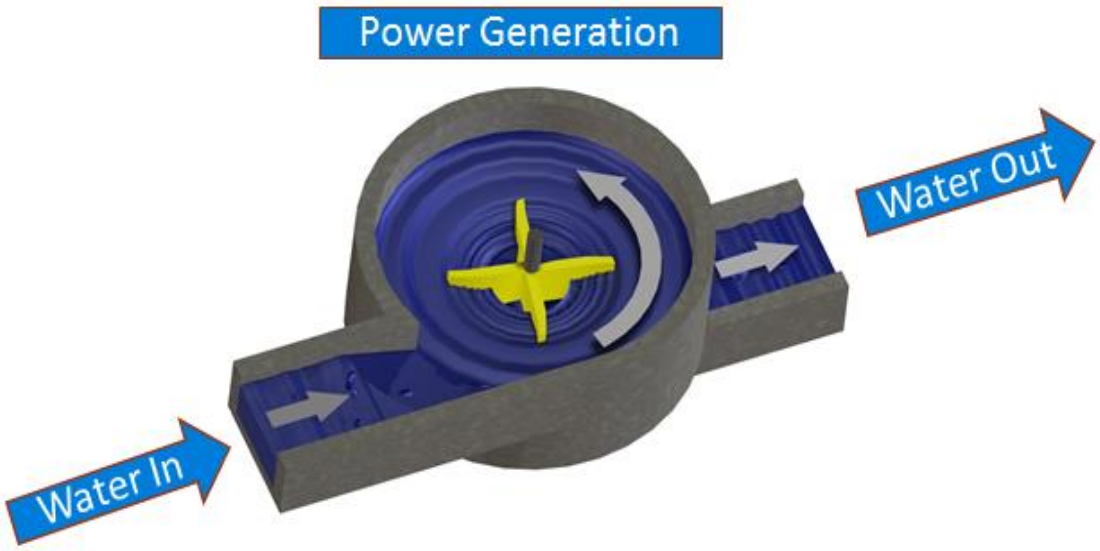

Figure 1. 5 Schematic of GWVPP [**21**]

GWVPP was first installed in Obergrafendorf, Austria. The turbine was patented by its inventor in 2004. The plant had a discharge of 1 m^3/s and a total head of 1.3m. The recorded efficiency of the plant was upto 80%. This plant was capable of generating power up to 10 kW. [**22**]

In this system, the energy contained within an artificially induced large water vortex over a small head is harnessed. Water flows tangentially into a cylindrical basin with an orifice at the bottom as shown in Figure 1.5. The combined effect of the localized low pressure at the orifice and the circulation which is induced as a result of the tangential entry through inlet, causes the water to restructure into a vortex like flow pattern [**9**]. The potential energy of the entering water is entirely converted to kinetic energy which can be extracted from it by the use of coaxial turbine which has a vertical axis.

All the micro-hydro power plants have certain advantages over each other. But the GWVPP has certain advantages over all other types of micro-hydro power-plants such as:

i. It operates at a low rpm and does not cut the natural stream of water therefore it does not harm the aquatic and marine life **[23] [24]**.

ii. It increases the water surface area and thus enhances the process of aeration therefore it is useful for the aquatic life as compared to its

contemporaries, which depletes the water quality and also cut the natural stream of water [**25**]

iii. It is easy to install and the return on investment starts after a very short time [**21**].

iv. It does not produce any harmful pollutants [**11**].

v. It considerably increases the flow velocity of the water without any external effort [**25**].

vi. It is better in terms of power generation since the water acts on all the blades at the same time [**9**].

vii. It can be installed along the run of the river, so there is no need for dam construction [**13**].

viii. The installation costs and transmission losses associated with long transmission lines are minimized.

ix. It has very simple and few moving parts so serviceability and operating costs are low.

x. Parts can be manufactured locally.

xi. It is a low head (0.7m - 3m) micro-hydro turbine and can be easily installed on irrigation canals and rivers [**23**].

xii. This type of power plant does not require a large water storage reservoir [**26**]

xiii. For the same flow conditions, GWVPPs produce more output power as compared to other micro-hydro power plants [**9**].

xiv. A number of such turbines can be installed on the same river in cascaded form, in such a way that they do not affect the flow of the following turbines in the system as shown in Figure 1.6. [**21**]

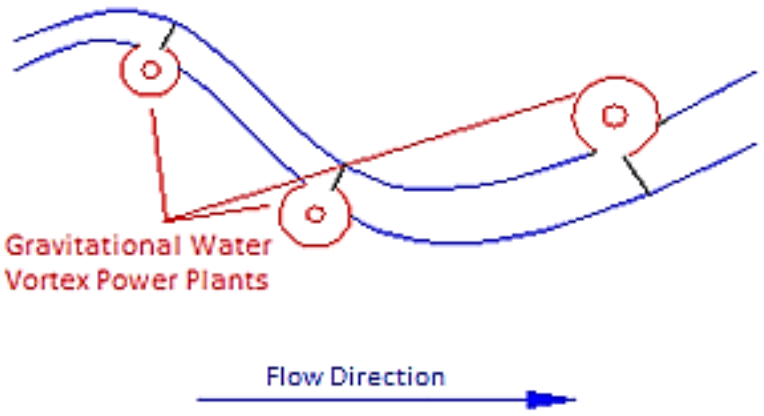

Figure 1. 6 Schematic for the cascaded system of GWVPP [**21**]

1.5 MOTIVATION

A lot of work has been done on the formation, influencing factors, analysis and study of vortices [27] [28] [29] [30] [31] [32] [33] [34] [35] [36] [18] [17]. But despite the easy installation of GWVPPs, their lower construction cost [21], high efficiency [37] [38], easy maintenance [21] and an excessive potential, due attention has not been paid to them.

A few of the studies on the GVWPP have been discussed in the following paragraphs:

Aravind Venukumar [9] experimentally demonstrated how the power produced using GWVPP is more than that obtainable if any other conventional power plant is used instead of this plant.

Omar Yaakob et al. [14] set up a gravitational water vortex pool for efficient extraction of energy from water. ANSYS Fluent was used to investigate the optimum vortex pool configuration. The efficiency of the setup was found to be around 40% between 28 and 38 rpm.

Dhakal et al. [39] used ANSYS Fluent for the analysis of different basin geometries for the vortex formation and for the measurement of velocities. They proposed that the optimum position of runner in the vortex plant is 65% from the top of vortex, since this is the point where maximum velocities can be achieved.

Wanchat and Suntivarakorn [40], [41] used Computational Fluid Dynamics (CFD) to simulate the vortices formed in three different types of basin geometries. They suggested that the most suitable configuration for a gravitational water vortex pool is a cylindrical tank with an orifice at the bottom center. The diameter of the orifice should be from 14% to 18% of the tank diameter. They also performed experimental validation of the numerical results using five blades. The efficiency of the plant was 30%.

Dhakal et al. [42] conducted experimental investigation of the GWVPP using turbine models of 3, 6 and 12 conical blades to find the optimum number of blades for the plant. The maximum efficiency of the plant was found to be 29.63%. The efficiency decreased with increase in number of blades since they caused a greater distortion in the vortex. The efficiency also decreases with increase in radii of the blades since the water velocities at radii far away from the core are lower.

Power et al. [43] performed a detailed experimental investigation of the effects of varying flow rates, inlet conditions, blade sizes and blade numbers on the turbine

speed, torque and vortex height. A maximum efficiency of 15.1 % was obtained. This efficiency was calculated at the maximum flow rate and using the inlet head of 0.25 m. Increasing the blade diameter caused an increase in the efficiency and the same trend in efficiency was observed when the number of blades was increased for the tested configurations. The output power increased with increasing the flow rates and when the resisting force on the blades was considerably increased.

Singh et al. [**37**], [**38**] completely modified the layout of GWVPP by using guide vanes as the stator and the blades as the rotor. The guide vanes directed the water at 47^{o} angle and thus restricting the radial and tangential velocity components at the blade inlet from varying with load variations. Their blade optimization methodology includes increase of efficiency by reducing the discharge through the turbine.

To much extent, the vortex formation has been explained fairly, but the studies on the parameters that affect the vortex formation in basins is scrace. Negligible work has been done on the basin aspect ratios, inlet width and inlet depth. Moreover, different authors used different blade profiles for the extraction of energy using GWVPP, but most of the authors did not perform experimental validation of their models. Moreover many authors relied on a single-phase simulation for their analysis, while in reality the effect of air can not be ignored in a GWVPP. Due to the afore mentioned reasons, this research focuses on the parametric analysis of the basin and a comparative analysis of the performance of different blade profiles and their experimental validation under the same conditions.

1.6 AIM AND OBJECTIVES

1.6.1 AIM

The aim of the study is to optimize the GWVPP by comparing the efficiencies of four different types of blade profiles.

1.6.2 OBJECTIVES

The objectives of the study include:

i. Parametric analysis of the basin
ii. Multi-phase numerical analysis vortex formation in GWVPP.
iii. Analysis of vortex distortion caused by blades due to different load conditions.
iv. The determination of most suitable basin configuration for the given head and discharge conditions.

v. The numerical analysis of efficiency of different blade profiles for GWVPP

1.7 STRUCTURE OF THESIS

Chapter 1 introduces the concept of GWVPP, its working mechanism and its origin. The chapter also defines the methodology adopted for the optimization of the plant using CFX.

Chapter 2 describes the approach used for the designing of the basin and the blades, and the steps performed in order to obtain the numerical results of basin analysis and the torques generated when different blade geometries were analyzed in ANSYS CFX.

Chapter 3 describes the numerical results obtained for the parametric analysis of the basin and the performance analysis of different blade profiles.

Chapter 4 describes the experimental setup and the results obtained when the basin and blade geometries were analyzed experimentally. This chapter also illustrates the comparison of the numerical results against the experimental results and validates the use of selected methodology for the analysis of GWVPP.

Chapter 5 concludes the numerical and experimental results and contains future recommendations that may help in obtaining better values of efficiencies and will result in minimizing the range of error between numerical and experimental results.

1.8 METHODOLOGY

Figure 1. 7 illustrates the methodology adopted for the optimization of blades using ANSYS CFX. The numerical part of the research has been divided into two phases, the first phase is the basin optimization, while the second phase is the blade optimization, followed by experimental validation of the results.

Literature review helped in the designing of the basin. The basin was further optimized numerically for the production of air-core. After the optimization of the basin, different blade designs were placed in the optimized basin for the performance analysis using ANSYS CFX. An experimental setup was fabricated for the validation of numerical results and the numerical and experimental results were compared. This finally led to the selection of optimum blade profile for use in gravitational water vortex pool.

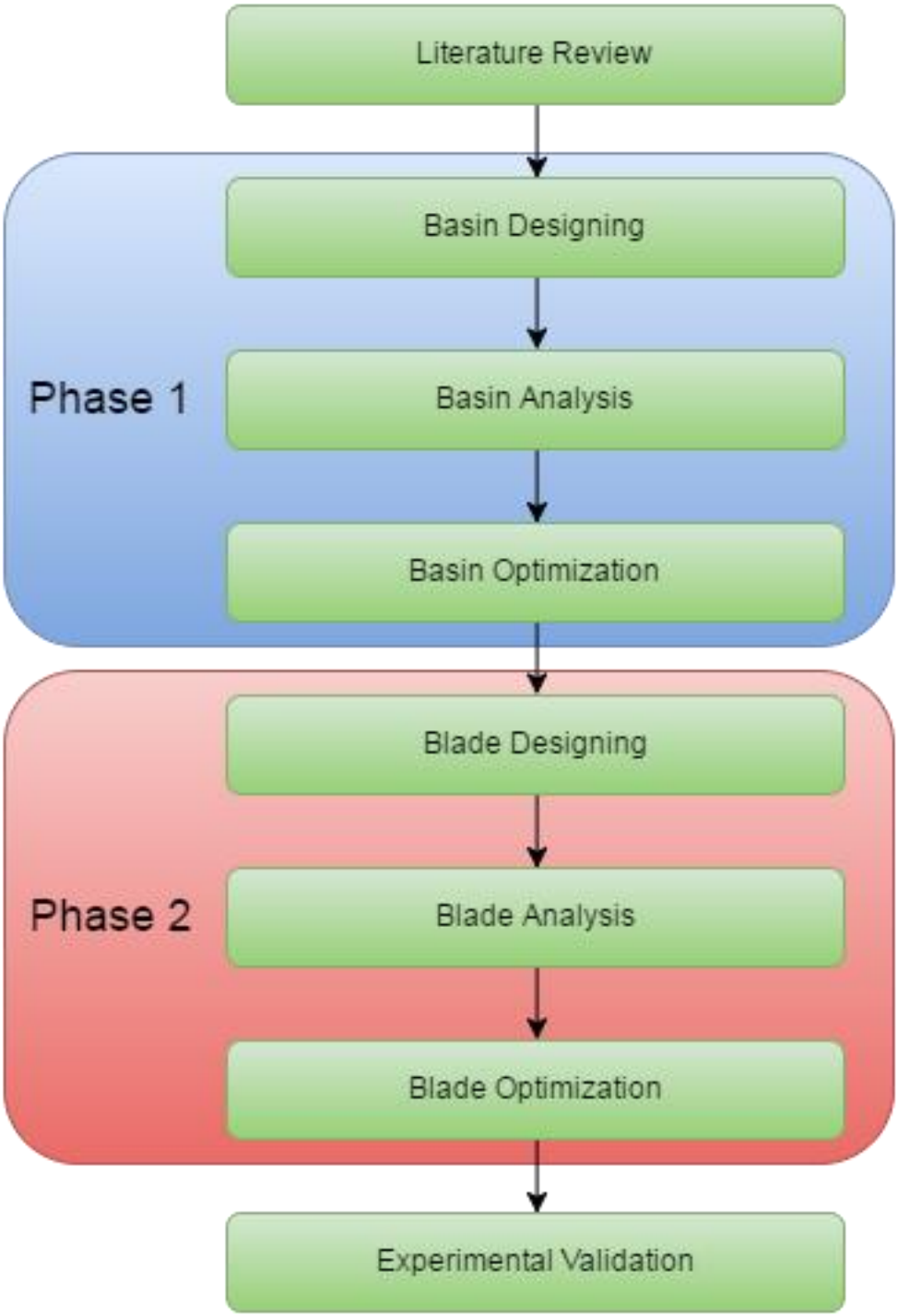

Figure 1. 7 Methodology for Blade Optimization

CHAPTER 2. DESIGN AND ANALYSIS

2.1 ANALYSIS METHODOLOGY

The methodology adopted for the CFD analysis and optimization of the GWVPP is illustated in Figure 2.1.

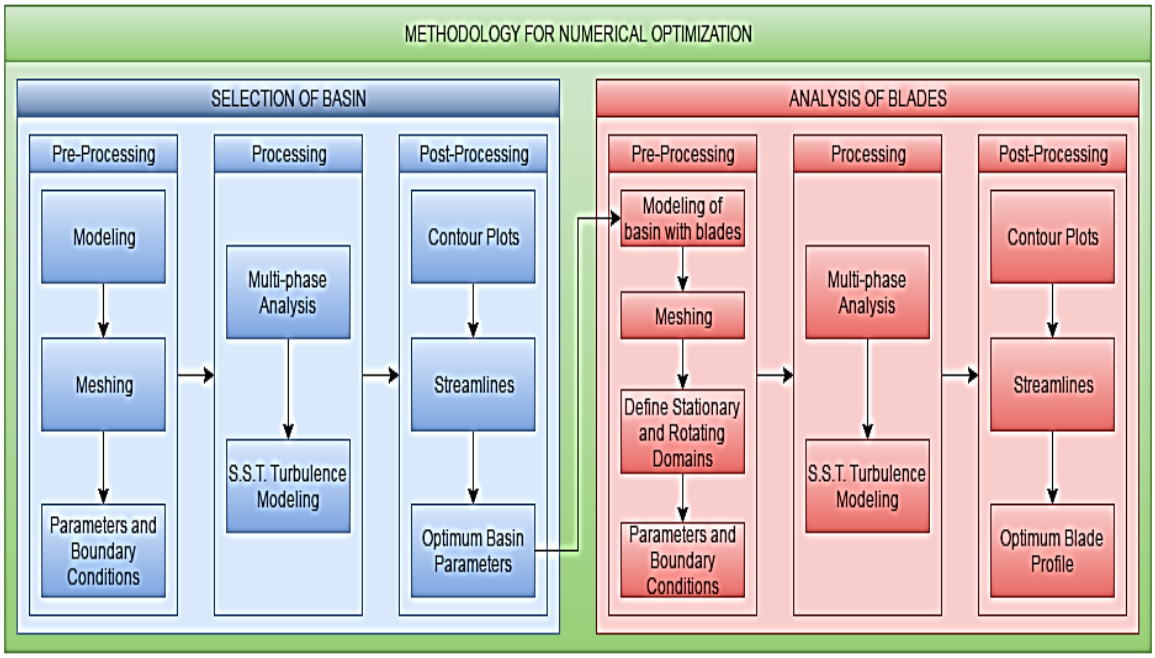

Figure 2. 1 Methodology for Numerical Optimization of Blades

The numerical optimization may be divided into two steps. The first step is the selection of a basin which has a full air-core vortex and higher gain in tangential velocities, along with a reasonable height of the vortex. The second step is the comparison of four blade shapes to achieve maximum output power. This comparison yields the optimum blade shape for use in GWVPP.

2.2 SELECTION OF BASIN

2.2.1 DESIGNING OF BASIN

Wanchat and Suntivarakorn [**40**] [**41**] suggested that a cylindrical tank with a discharge hole at the bottom center was the most suitable configuration to generate a water vortex along with a tangential water entry into the basin. They also suggested that the optimum basin diameter to outlet diameter ratio is 0.14 to 0.18 [**41**]. This led to the designing of the basin. When the mean tangential velocity of water in a vortex basin increases, the water motion becomes tangential instead of axial and the height of the vortex increases, thereby increasing the vortex strength [**31**] [**41**] [**28**]. Therefore, focus was put on the designing of a basin that generates a free surface air core vortex,

with maximum possible height and higher velocities at the core of the vortex. For this purpose, a reference basin was designed whose dimensions are shown in Table 2.1.

Table 2. 1 Dimensions of Reference Basin

Basin Parameter	Reference Value(mm)
Basin Diameter	500
Basin Height	500
Outlet Diameter	70
Inlet Width	150
Inlet Depth	150

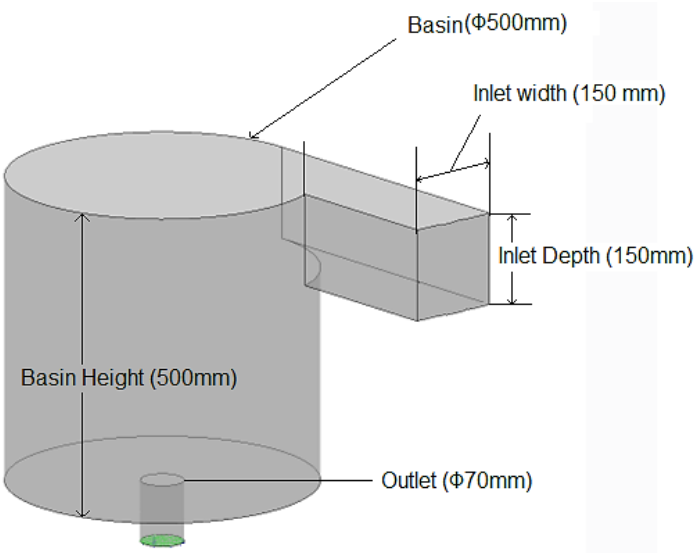

Figure 2. 2 Reference Basin

To increase the vortex strength, the vortex dependency parameters of the basin geometry are varied from the reference values (given in Table 2.1) one by one while keeping all others constant and are analyzed for the tangential velocities of the water in the vortex core, vortex height and the quality of air core ranging from 0 (for no air-core) to 1 (for full air-core). Besides varying the geometry parameters, the flow conditions are also varied to analyze the effect of flow velocities on the vortex formation. Since vortices with fully developed air-core have higher potential for power production as compared to those which do not have a fully developed air core, therefore, formation of air core was also focused during the selection of basin.

The parameters that are analyzed for the effect on the vortex and the tangential velocities are:

i. Basin Diameter (0.4m to 0.8m)
ii. Outlet/Basin Diameter (0.13 to 0.17)

iii. Basin Height to Diameter Ratio (0.5 to 1.5)

iv. Inlet Channel Width Ratio (0.1 to 0.5)

v. Inlet Channel Depth Ratio (0.1 to 0.5)

vi. Inlet Velocity (0.1 to 0.6 m/s)

Different cases that were analyzed in this research are shown in Table 2. 2.

Table 2. 2 Sets of values used for basin analysis

Sr. No	Basin Diamter	Basin dia./ outlet dia. ratio	Basin Height	Aspect Ratio (D/H)	Inlet Width	Inlet Depth	Flow Velocity	Mass Flow
	mm		mm		mm	mm	m/s	kg/s
1	500	0.14	500	1	150	150	0.1	2.5
2	500	0.14	500	1	150	150	0.2	5.0
3	500	0.14	500	1	150	150	0.3	7.5
4	500	0.14	500	1	150	150	0.4	10.0
5	500	0.14	500	1	150	150	0.6	12.5
6	500	0.14	500	1	150	50	0.3	2.5
7	500	0.14	500	1	150	100	0.3	5.0
8	500	0.14	500	1	150	150	0.3	7.5
9	500	0.14	500	1	150	200	0.3	10.0
10	500	0.14	500	1	150	250	0.3	12.5
11	500	0.14	500	1	50	150	0.3	2.5
12	500	0.14	500	1	100	150	0.3	5.0
13	500	0.14	500	1	150	150	0.3	7.5
14	500	0.14	500	1	200	150	0.3	10.0
15	500	0.14	500	1	250	150	0.3	12.5
16	500	0.14	250	0.5	150	150	0.3	7.5
17	500	0.14	375	0.75	150	150	0.3	7.5
18	500	0.14	500	1	150	150	0.3	7.5
19	500	0.14	625	1.25	150	150	0.3	7.5
20	500	0.14	750	1.5	150	150	0.3	7.5
21	500	0.13	500	1	150	150	0.3	7.5
22	500	0.14	500	1	150	150	0.3	7.5
23	500	0.15	500	1	150	150	0.3	7.5
24	500	0.16	500	1	150	150	0.3	7.5
25	500	0.17	500	1	150	150	0.3	7.5
26	400	0.20	500	0.8	150	150	0.3	7.5
27	500	0.16	500	1	150	150	0.3	7.5
28	600	0.13	500	1.2	150	150	0.3	7.5
29	700	0.11	500	1.4	150	150	0.3	7.5
30	800	0.10	500	1.6	150	150	0.3	7.5

Using the above methodology, the reference basin was optimized to generate a full air core vortex, (the one in which the air core is fully developed) along with a

considerable increase in the kinetic head. The dimensions of the optimized basin are given in Table 2. 3, while the optimization procedure is discussed in Section 3.1.7.

Table 2. 3 Optimized Values of Basin Parameters

Basin Parameter	Optimized Value(mm)
Basin Diameter	500
Basin Height	500
Outlet Diameter	80
Inlet Width	100
Inlet Depth	100

2.2.2 MODELING OF THE BASIN

All the basins were modeled in ANSYS CFX Design Modeler ® as a solid model. A model of the reference basin and the optimized basin are shown in Figure 2. 3 (a) and (b) respectively.

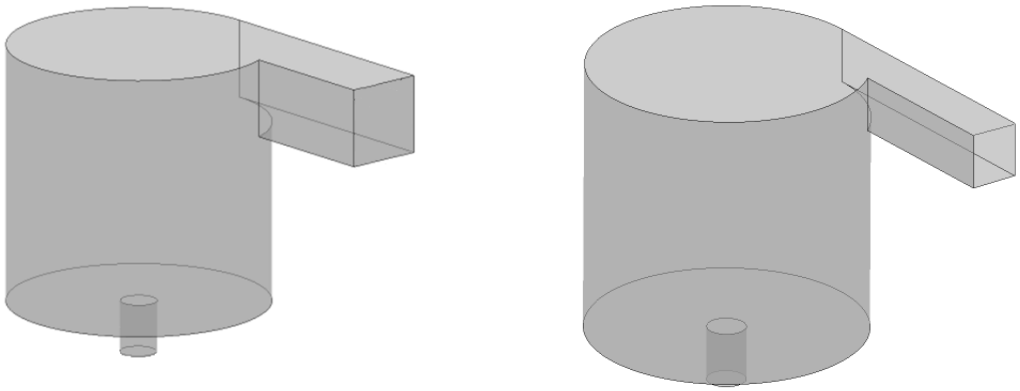

(a) Reference Basin (b) Optimized Basin

Figure 2. 3 Basin Models (a) and (b)

2.2.3 MESHING OF THE BASIN

Since all the basin geometries were having different parameters, therefore automatic meshing of the basin was done using tetrahedral elements in ICEM ® CFD to create finite regular blocks. Mesh sensitivity analysis was also carried out for all the basins. The convergence criteria selected for mesh sensitivity analysis was based on the outlet velocity and the net mass flow into and out of the basin and convergence upto 0.3% was aimed, since this is a reasonable value as far as multiple fluids are concerned. The meshes of the reference and the optimized basin are shown in Figure 2. 4 (a) and (b). the number of elements used are 8159432 and the element size for the mesh is 0.001. Tetrahedral elements are used for the meshing of basin.

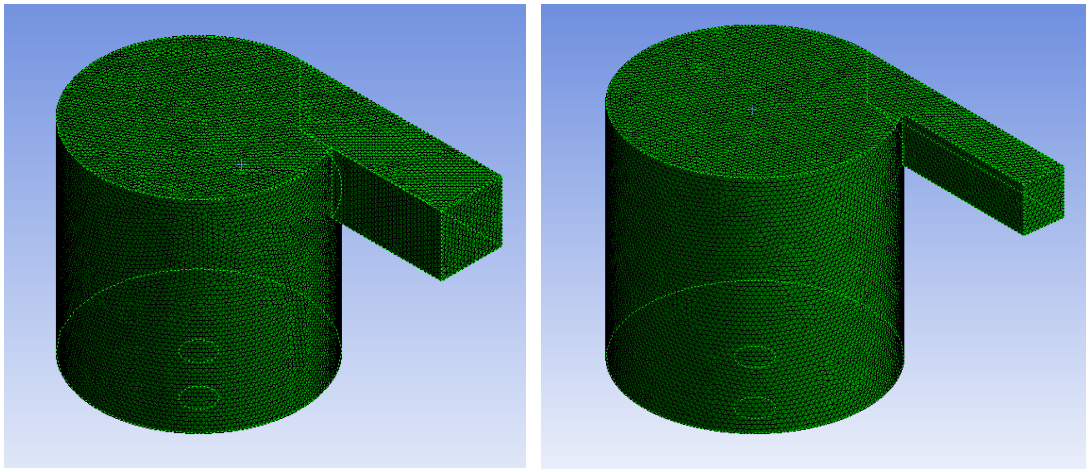

(a) Reference Basin (b) Optimized Basin

Figure 2. 4. Basin Meshing

2.3 SELECTION OF BLADES

Four blade profiles were analyzed for the power production and vortex distortion in the gravitational water vortex basin using ANSYS CFX ®. The selection of the blade profiles was based on the researchwork of different authors **[9]** **[23]** **[39]** and **[42]**. These shapes are as follows and are shown in Figure 2. 5.

Inverted Conical Blades ➔ Profile 1

Cross Flow Blades ➔ Profile 2

Curved Rectangular Blades ➔ Profile 3

Twisted Blades ➔ Profile 4

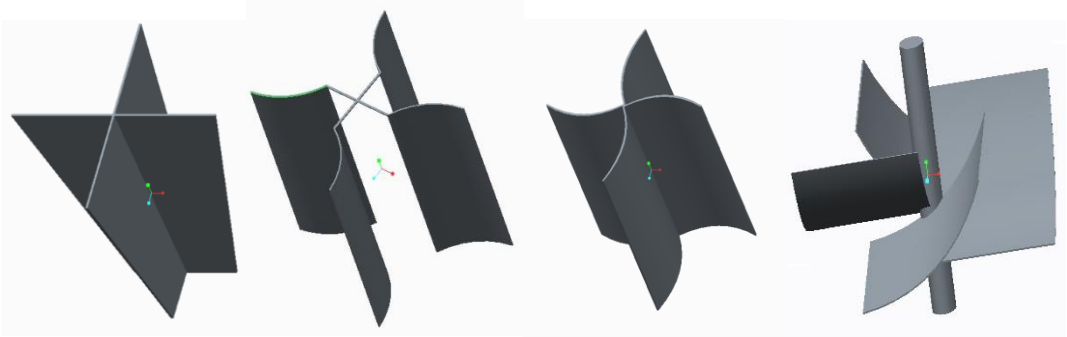

(a) Profile 1 (b) Profile 2 (c) Profile 3 (d) Profile 4

Figure 2. 5 Blade Profiles

2.3.1 DESIGNING OF BLADES

The dimensions of the selected blades are completely dependent on the vortex formed in a particular basin. For the designing of these blades, the vortex profile was analyzed which ultimately led to the designing of the blades.

In a vortex the layers of fluid flow are in a spiral manner, with tangential velocities greater than the radial and the axial velocities with the optimum position for the blade installation at 35% of the vortex height from the bottom of the vortex [**42**]. Keeping in view the vortex profile as shown in Figure 2.6, the outer diameter of the blades was selected such that it should not be less than the minimum distance between the water surfaces on both sides of the blade, at a position of 35% from the bottom of the basin. This arrangement enables the water to transfer maximum kinetic energy to the blades for the generation of power.

The designing of conical blades (Profile 1) is shown in Figure 2. 6. This was the most different blade profile since the blade radius decreses as we move towards the basin bottom. This causes a complexity when the vortex height is reduced with the decrease in angular velocity of the rotating blades.

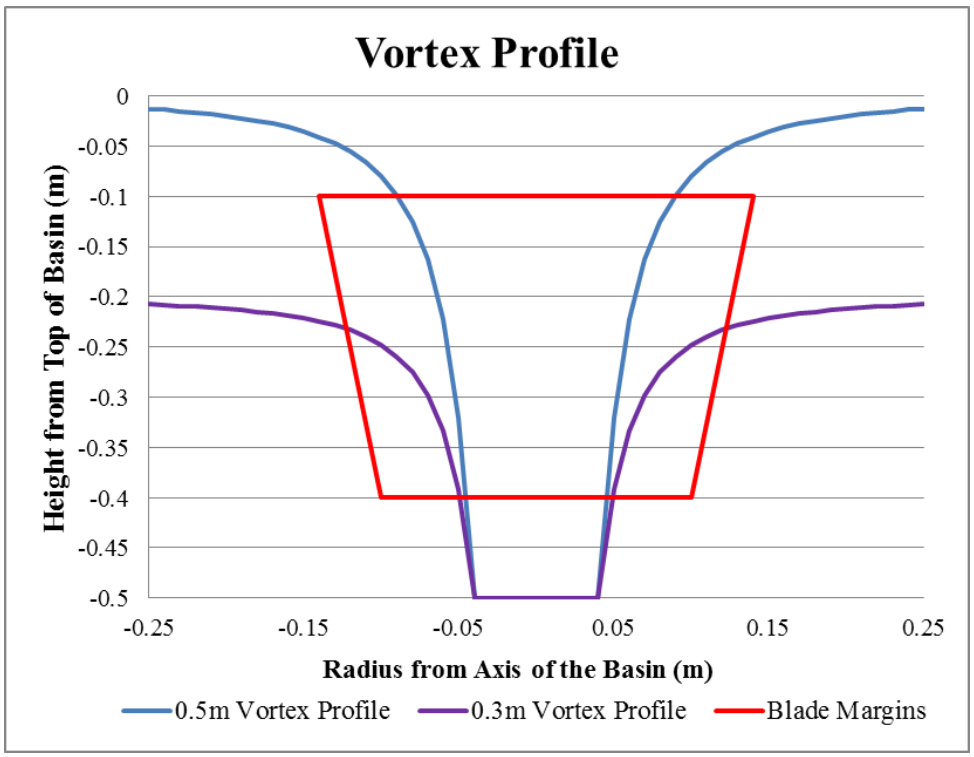

Figure 2. 6 Designing of Conical Blades

The drawings of all the blades are attached at the end of the thesis as Appendix A.

2.3.2 MODELING OF THE BLADES

To enable rotation of the blades in the basin, the basin was divided into two domains. An outer stationary domain, referred to as the basin domain as shown in Figure 2. 7(a) and a central cylindrical rotating domain, which contained the blades, referred to as the blade domain as shown in Figure 2. 7(b). The formation of the blade domain

enables the symmetric rotation of the blades without effecting the stationary position of the basin domain. All blades are modeled in Pro-Engineer software and imported into the ANSYS CFX ® using the “Cut Material Option”. The use of this option treats the blade as walls inside the rotating blade domain as shown in Figure 2. 8. The position of the blade walls inside the cylindrical domain was selected so as to keep the blade at a height of 100 mm above the base of the basin walls. This was done to ensure the submergence of blade in the vortex at all vortex heights. The assembly of the basin domain and the blade domain is shown in Figure 2. 8.

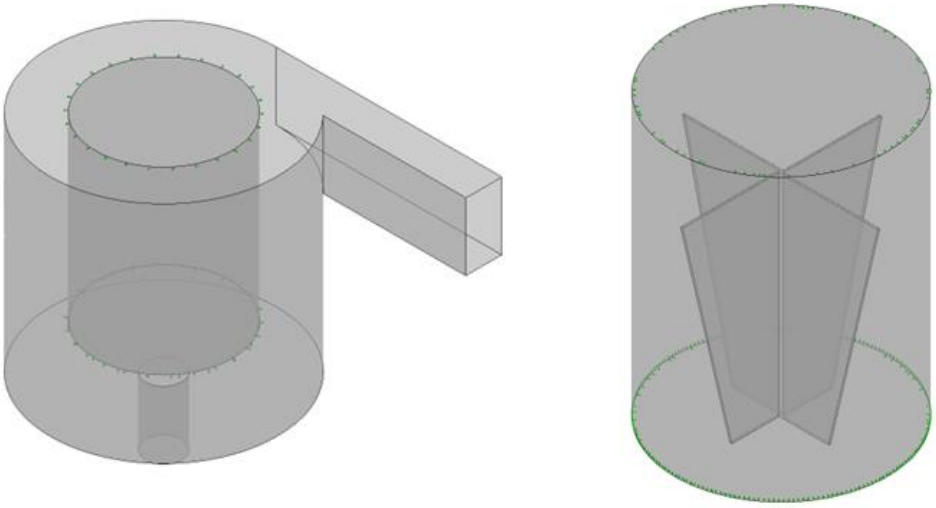

(a) Basin Domain (b) Blade Domain

Figure 2. 7 Domains (a) and (b)

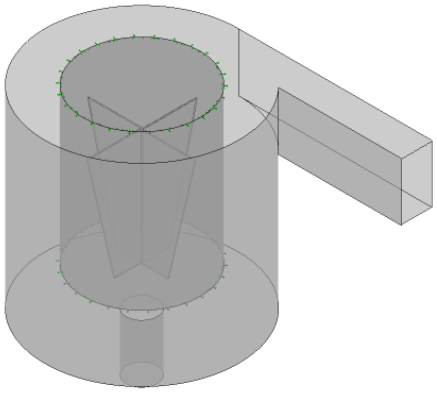

Figure 2. 8 Assembly of the basin domain and blade domain

2.3.3 MESHING OF THE BLADES

Utilizing the ANSYS built in feature of automatically optimizing the mesh structure, meshing of the blades is done using automatic tetrahedral mesh elements in ICEM ® to create finite smooth transition blocks with high refinement on walls to obtain the final mesh. The mesh on the blades was even more refined to get better results. Meshing on the blade surfaces was refined upto 5 layers as suggested by Riccardo Ferreira [**44**]. Mesh sensitivity analysis of the basin domain was performed based upon the mass flow and the velocity of water, while mesh sensitivity analysis of the blade domain was based on the torques on the blade surfaces [**45**]. The meshing of the blade domain is shown in Figure 2. 9. The types of elements used in both these domains are tetrahedral. The number of elements used for the basin domain are 4816342 while for blade domain, the number of elements used are 8922533. The element size in both the domains is 0.001 with a refinement of 5 layers at the blade surface.

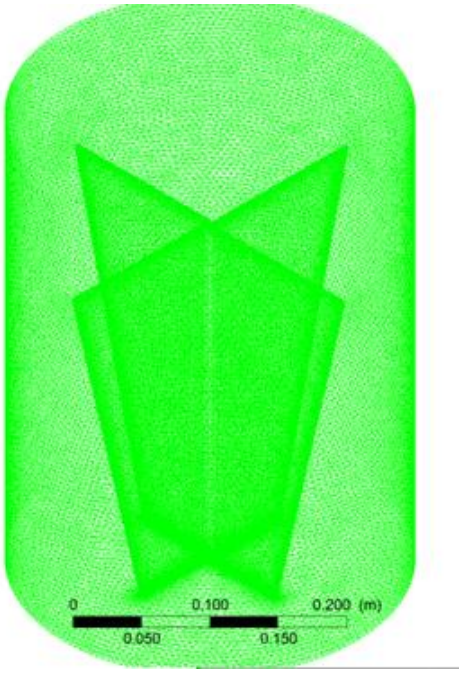

Figure 2. 9 Blade Domain Meshing

2.4 ANALYSIS

The free surface air core vortex is formed as a result of the interface between air and water [**35**] [**40**], therefore the analysis is based on multiphase Eulerian fluid approach in which two fluids, air and water, occupy the same domain and same velocity fields. The temperature of the domain is set to 25^0C and the reference pressure is set to 1atm.

The buoyancy reference density is set to the density of air at 25^0C, which is equal to 1.185 kg/m^3.

2.4.1 GOVERNING EQUATIONS

The governing equations for the vortex, which is a steady, incompressible, viscous and turbulent flow; are the Continuity Equation and the Navier Stokes Equations, which are described in cylindrical co-ordinates as follows [**20**] [**32**]:

$$\frac{\partial V_r}{\partial r} + \frac{\partial V_z}{\partial z} + \frac{V_r}{r} = 0 \quad (1)$$

$$\partial V_r \frac{\partial V_\theta}{\partial r} + Vz \frac{\partial V_\theta}{\partial z} - \frac{V_r V_\theta}{r} = \nu\left(\frac{\partial^2 V_\theta}{\partial r^2} + \frac{\partial V_\theta}{r\partial r} - \frac{V_\theta}{r^2} + \frac{\partial^2 V_\theta}{\partial z^2}\right) \quad (2)$$

$$V_r \frac{\partial V_r}{\partial r} + Vz \frac{\partial V_r}{\partial z} - \frac{V_\theta^2}{r} + \frac{\partial \rho}{\rho \partial r} = \nu\left(\frac{\partial^2 V_r}{\partial r^2} + \frac{\partial V_r}{r\partial r} - \frac{V_r}{r^2} + \frac{\partial^2 V_r}{\partial z^2}\right) \quad (3)$$

$$\partial V_r \frac{\partial V_z}{\partial r} + Vz \frac{\partial V_z}{\partial z} + \frac{\partial \rho}{\rho \partial z} = g + \nu\left(\frac{\partial^2 V_z}{\partial r^2} + \frac{\partial V_z}{r\partial r} + \frac{\partial^2 V_r}{\partial z^2}\right) \quad (4)$$

Where V_r, V_θ and V_z are the radial, tangential and axial velocities respectively, g is the gravitational acceleration, ν is the Kinematic viscosity and ρ is the density of the fluid.

Due to the complexity of the equations, it is almost impossible to solve the equations analytically. Moreover, the presence of multiple domains takes the analytic solution of these equations to a higher difficulty level. Due to this reason, ANSYS CFX was employed for the solution of these equations.

2.5 SIMULATION PARAMETERS

The common simulation parameters for the analysis of basin and analysis of the blades are discussed in the following sections. In case of basin analysis, there is no blade domain, so the boundary conditions used are only those of the basin domain

Since the air core vortex is a result of the air-water interface, therefore two fluids are defined for the analysis. The two fluids are air and water. Built-in fluid models are used for both fluids. The properties of water and air are taken at 25^0C and 1atm pressure. Since the entire runner is not fully immersed in the water and hence air is present inside the runner in the regions that are not submerged in water, therefore a multiphase simulation is required for the simulation of vortex and the turbine. In the production of air-core vortices, the buoyancy plays a vital role, therefore, buoyancy is also included in the analysis.

Turbulence models based on *k-ω* were designed to give accurate predictions on separating flows under adverse pressure gradients [**46**]. The Shear Stress Transport

(SST) model was developed to overcome the deficiencies in the *k-ω* and Baseline *k-ω* models. The use of k-ω formulation makes the turbulence model usable for inner parts of boundary layer, as well as for near-wall regions. Therefore the use of SST model over other models is preferred [**46**]

Chen et al. [**47**] performed a comparison of RNG k-ε Turbulence Model and Standard k-ε Turbulence Models and concluded that RNG k-ε Turbulence Model is more suitable for the simulation of air core vortices as compared to the Standard k-ε Turbulence Model due to the great curving streamline flows. Omar Yaqub et al. [**14**] used The SST Model to simulate the artificial vortex for a micro-hydro power plant using multiphase Eulerian fluid approach and performed experimental validation of the obtained results. S. R. Shah et al. [**48**] suggested the use of Reynolds Averaged Navier Stokes Equations together with k-ω SST Turbulence Model over RNG k-ε Turbulence Model, since the k-ω SST Turbulence Model provided better results in comparison to RNG k-ε Turbulence Model.

In the initializing of the domains, identification of the domains as stationary or rotating is required. The basin domain is the fluid domain and it is the stationary domain. Since the blades are the rotating components in the assembly, therefore the blade domain is the rotating fluid domain and its rotational speed is an input parameter in the analysis. The rotational speed of the domain is set at increments of 25 rpms starting from 50 rpm up to 200 rpm. The domain is set as isothermal.

At the inlet, different velocities ranging between 0.1 m/s and 0.5 m/s were selected keeping in view the size of the reference basin. For velocities greater than this range, the basin diameter has to be increased along with an increase of outlet diameter. The water inlet velocity for the blade analysis was fixed at 0.45 m/s which was obtained by testing the optimized basin at various velocities. Multiphase domain was defined for all the analyses, since water and air both are present in the basin. Atmospheric pressure and conditions are applied at the upper surface of the basin as well as for the bottom drain. The boundary conditions at the inlet, outlet and at the upper surface of the basin are defined as:

- Inlet: Normal velocity with α_{air}:0 and α_{water}:1
- Outlet: Opening with opening pressure and α_{air}:1 and α_{water}:0
- Upper surface: Opening with opening pressure and α_{air}:1 and α_{water}:0

Where α_{air} defines the volume fraction of air while α_{water} defines the volume fraction of water. These input parameters are valid for both cases: 1) without turbine blades and 2) with turbine blades. These conditions can be physically understood by considering the turbine when it is not operational. Only water is present at the inlet of the basin. At the same time, there is only air at the outlet of the basin and at the upper opening of the basin. The walls of the basin were set as rough walls with sand-grain roughness of 0.045 which is the sand grain roughness of the steel sheet used for experimental model.

For blade analysis the same boundary conditions were set as those for the basin analysis, with the blade domain set as a rotating fluid domain. Air and water were selected as the fluids that are present in the domains. This is shown in Figure 2. 10.

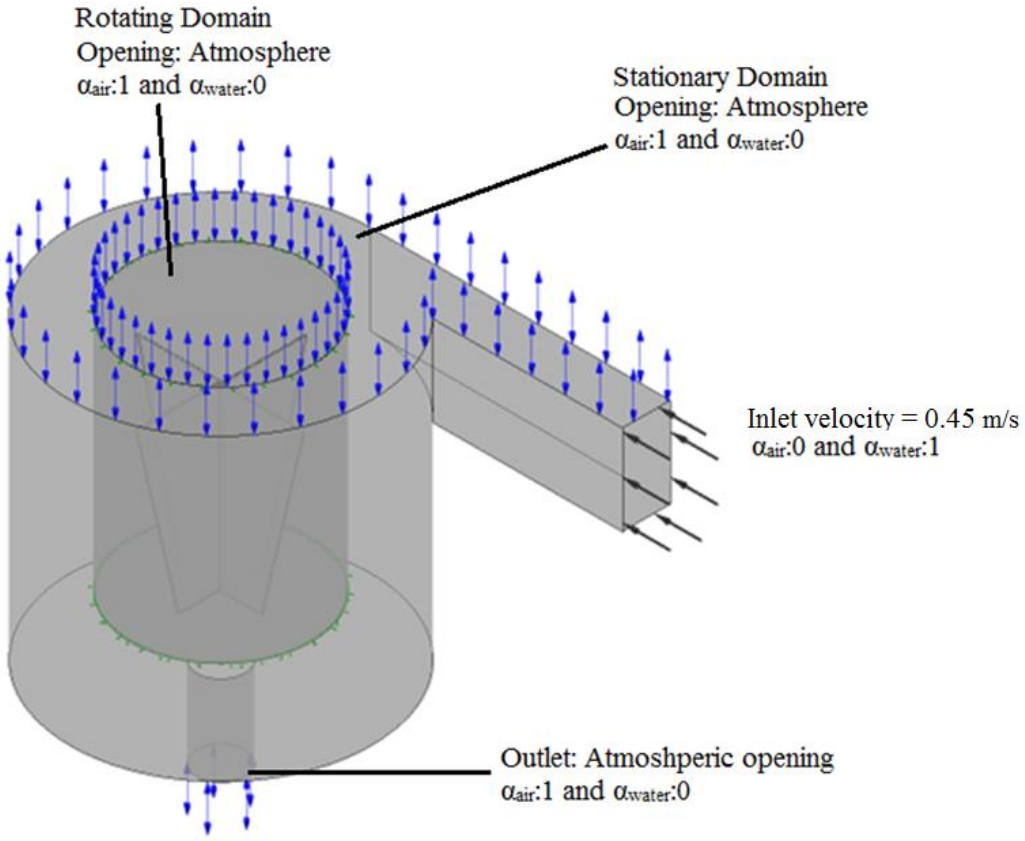

Figure 2. 10 Boundary Conditions for Blade Analysis

2.5.1 SOLVER PARAMETERS

Common solver parameters for both models include advection scheme as "High Resolution" and turbulence numeric was "First Order". Both of these options are set by default. Timescale was set to "Auto Timescale" with conservative length scale. This option selects the maximum possible time value above which the solution would

not converge. The no. of iterations was set to 300 while for some iterations where the fluid flow was not fully developed; the number of iterations was set ranging up to 500 with a residual target of 0.0001. It is very difficult to obtain a residual target below this value even after 800 iterations due to presence of multi-fluids.

2.5.2 OUTPUT PARAMETERS

CFX expression language is utilized to compute the efficiency of the turbine. For computing the efficiency in the CFX the following relations are used:

Average Vt on xy plane = ave(sqrt(Water.Velocity w^2))@xy plane

Average Vt on yz plane = ave(sqrt(Water.Velocity u^2))@yz plane

Average Vr on xy plane = ave(sqrt(Water.Velocity u^2))@xy plane

Average Vr on yz plane = ave(sqrt(Water.Velocity w^2))@yz plane

Average Va on xy plane = ave(sqrt(Water.Velocity v^2))@xy plane

Average Va on yz plane = ave(sqrt(Water.Velocity v^2))@yz plane

Mass flow Through Inlet = Water.massFlow()@Inlet

Mass flow Through Outlet = Water.massFlow()@Outlet

Max Vt on xy plane = maxVal(Water.Velocity w)@xy plane

Max Vt on yz plane = maxVal(Water.Velocity u)@yz plane

N (rpm) = Angular Velocity (input parameter)

*Omega (ω) =2*pi*N / 60*

Torque (T) = Torque on blade assembly

BHP = Brake Horse Power = Output Power = $T * \omega$

IHP = Input power w.r.t total head = γHQ

IHP2 = Input power wr.t. vortex height = γhQ

*η = efficiency w.r.t Total head = BHP/ IHP * 100*

*η_2 = efficiency wr.t. vortex height = BHP/ IHP2 * 100*

In case of any other turbine, the head H, is the net head of the inlet , but in case of GWVPPs, the head is actually the height of the vortex. This is because the water entry height above the vortex surface does not result in any positive effect on the vortex. Therefore, η_2 is also calculated for measuring the efficiency of the plant at any particular rpm.

The mass flow rate and the computed efficiency "η" is set in output monitor so that the stabilization of the mass flow rate and value of efficiency can be observed in the solution. While η_2 is calculated using iso-surface plots.

2.6 SIMULATION FLOW CHART

The complete simulation may be summarized in the form of a flow chart as shown in Figure 2.11.

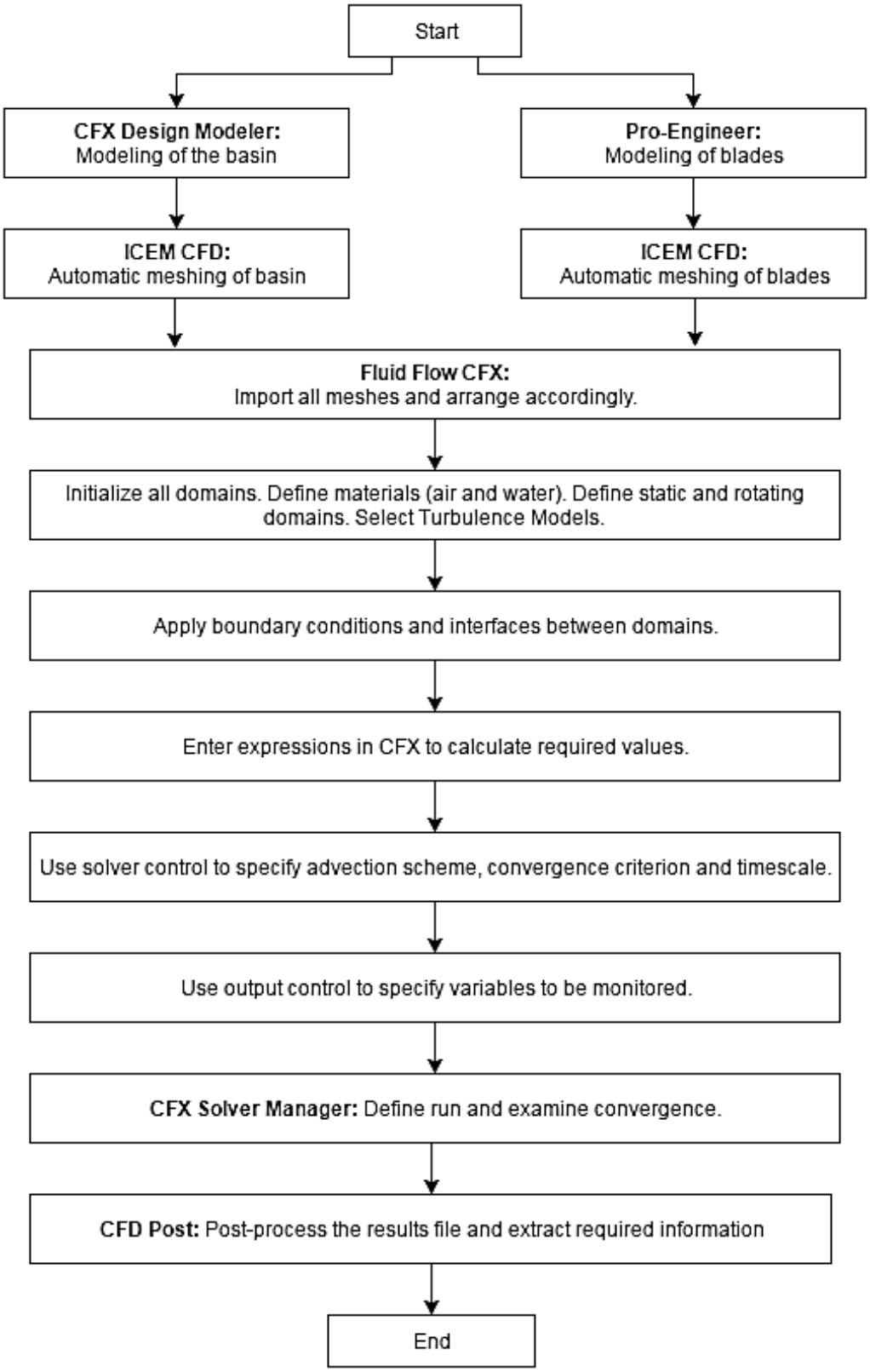

Figure 2. 11 Simulation Flow Chart

CHAPTER 3. RESULTS

Air core was not formed in the reference basin geometry and thus it is not suitable for use as gravitational vortex pool. The absence of air-core indicates that vortex is not formed properly and thus the power generated will be lesser if this basin is used. For this reason, the basin geometry was optimized using the results of basin analysis for air-core formation. The results obtained using reference basin geometry are shown in Figure 3. 1. The figure shows the vortex formed when the reference geometry was analyzed at a mass flow of 5.5 kg/s.

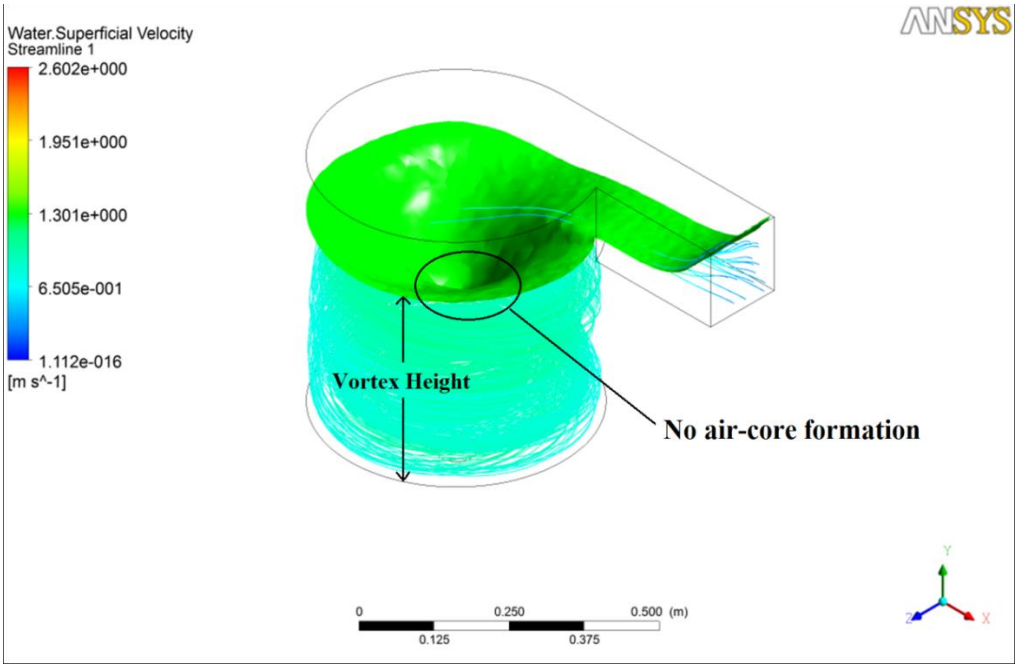

Figure 3. 1 Velocity streamlines and Fluid Flow in the initial/reference geometry

3.1 RESULTS OF BASIN ANALYSIS

The output parameters that were monitored during the basin analysis are height of vortex (H_v), the air-core formation (represented by Φ), gain in tangential velocity (ΔV_{tmax}), maximum tangential velocity (V_{tmax}), average tangential velocity (V_{tavg}), average radial velocity (V_{ravg}) and average axial velocity (V_{aavg}).

The formation of air-core was monitored throughout the cylindrical region of the basin, while other parameters were monitored by using two planes in xy and yz directions at the center of the basin and average of the values obtained by the two planes was used. The height of the planes was kept the same as the height of the basin, while the width of the planes was set equal to half of the basin diameter.

Air-core formation was observed in order to optimize the basin for vortex formation since a vortex with full air core has the tendency to produce higher power as compared to that without a full air core. The air core (represented by Φ) is a unitless parameter, which has been valued from Φ=0 to Φ=1. A value of Φ=0 indicates that air-core is not formed, while a value of Φ=1 indicates the presence of a fully developed air core that extends to the outlet of the basin.

Gain in tangential velocity was monitored in order to observe the relation between inlet velocity water and its velocity at the core of the radius. This was necessary as the increase in tangential velocity at inlet may possibly be accompanied by an increase in the tangential velocity at the air-core. The gain in tangential velocity (ΔV_{tmax}) is the percentage increase in maximum tangential velocity at the core. The maximimum tangential velocity (V_{tmax}) was monitored in order to check the effect of different parameters on the maximum velocity.

The flow out of the outlet causes a vortex to initiate at the free surface which gradually intensifies, causes the water rotation to speed up and in turn causes the pressure in the center of the vortex to decrease. This pressure gradually decreases to an extent that ultimately it reduces below the atmospheric pressure and sucks the air into the intake and forms an air core. The radius of the air core gradually reduces while moving from the free surface to the intake. The tangential velocity of the water in the vortex core is inversely proportional to the radius from the center of the vortex core; while the axial velocity depends directly on the depth inside the vortex core.

The results show variations in outputs and vortices formed under different basin parameters such as inlet velocity, basin height, outlet diameter, inlet channel width, inlet channel depth and mass flow rate. It is concluded that the optimized design parameters for the basin improves the efficiency of the plant to a significant extent by the generation of a strong vortex with air core. Different parameters effect the velocity in different ways, which are discussed in the following sections

3.1.1 EFFECT OF INLET VELOCITY

Increasing the inlet velocity causes an increase in the water height. The increase in water height can be attributed to the increased mass of water that enters the basin. The water height keeps on rising till the water overflows the walls of the basin. The rise of vortex height can be explained as “the mass flow out of the basin outlet increases till the vortex achieves a steady height when the water flow into and out of

the basin are equalized. The gain in tangential velocity is high when the inlet velocity is low and when a full air core is formed. With the distortion of the air-core, this velocity gain decreases. The increase in water height disturbs the critical submergence conditions and thus causes the air-core to diminish.

The rise of water level causes an increase in the exit velocity of the water at outlet, which ultimately increases the axial velocity. This increase continues till the water overflows the basin edges. Once overflow occurs, the tangential and axial velocities do not increase further. The overall change in radial velocity is almost negligible with respect to the change in inlet velocity. The trends observed with increasing the inlet velocity are shown in Figure 3. 2 and Figure 3. 3.

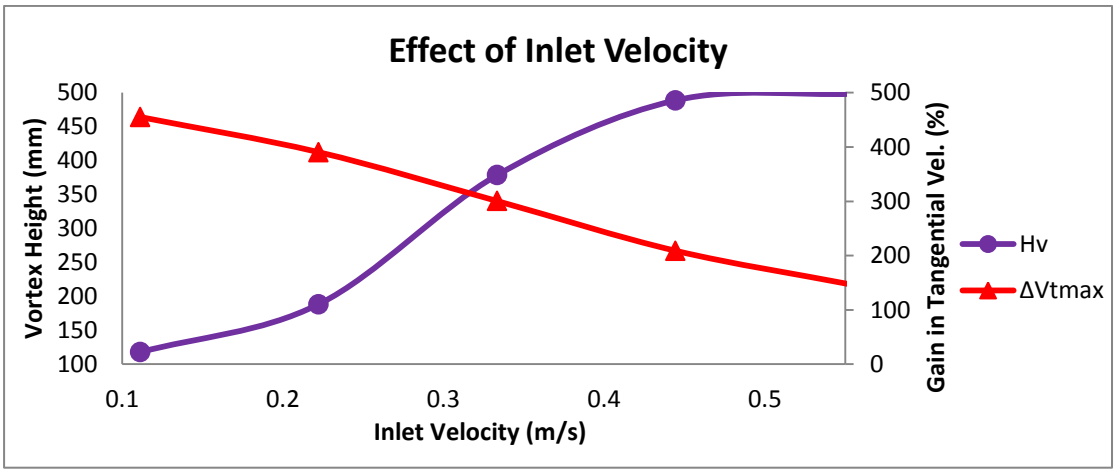

Figure 3. 2 Effect of Inlet Velocity on vortex height and gain in tangential velocity

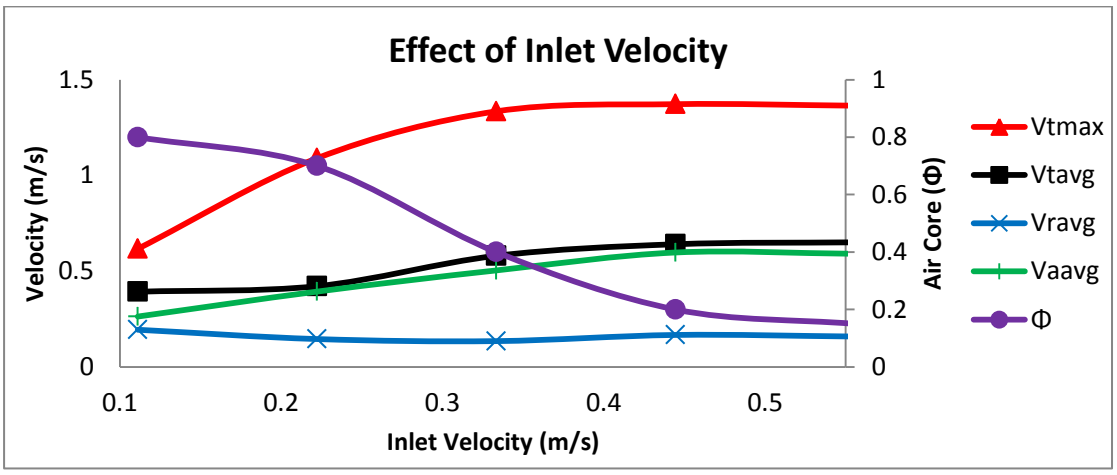

Figure 3. 3 Effect of Inlet Velocity on Air-core and Tangential, Radial and Axial Velocity.

3.1.2 EFFECT OF BASIN HEIGHT

The effect of basin height is measured in terms of aspect ratio. Aspect ratio is the ratio of basin height to the basin diameter. At lower aspect ratios, the water overflows the edges of the basin but the water height is lower than the critical submergence, and thus the air core is formed. The air core tends to diminish as the water height is increased in the basin. Tangential velocity at the air-core is maximum when the water enters the basin at a height just above the vortex height. This increase is due to the smooth entry of the water into the basin. Further increase in the basin height, and ultimately the inlet height does not produce any positive results. When the water drops from a height into the basin, the axial velocity increases due to gravity and the impact of the falling water on the tangentially moving water causes the tangential velocity to decrease. Increasing the basin height causes a decrease in the air core due to the disturbance in submergence of outlet away from the critical submergence.

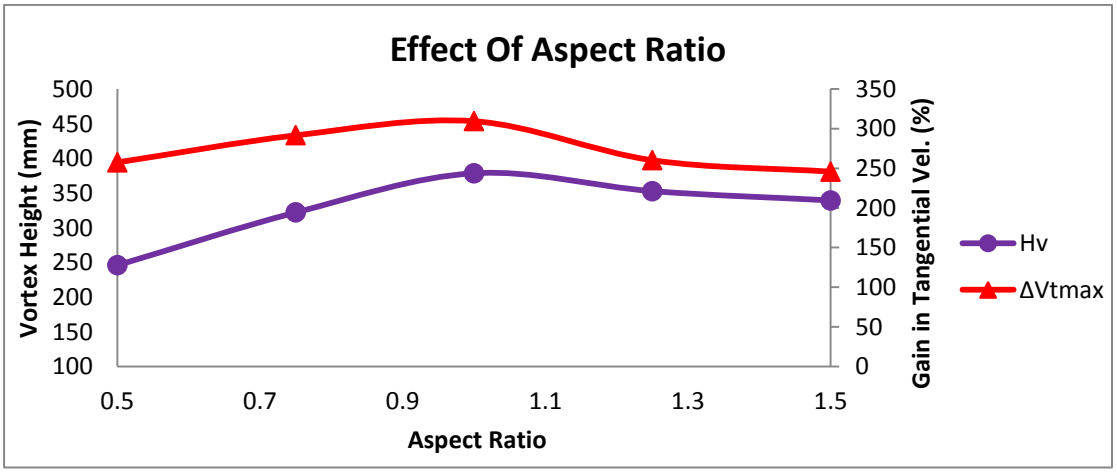

Figure 3. 4 Effect of Basin Height on vortex height and gain in tangential velocity

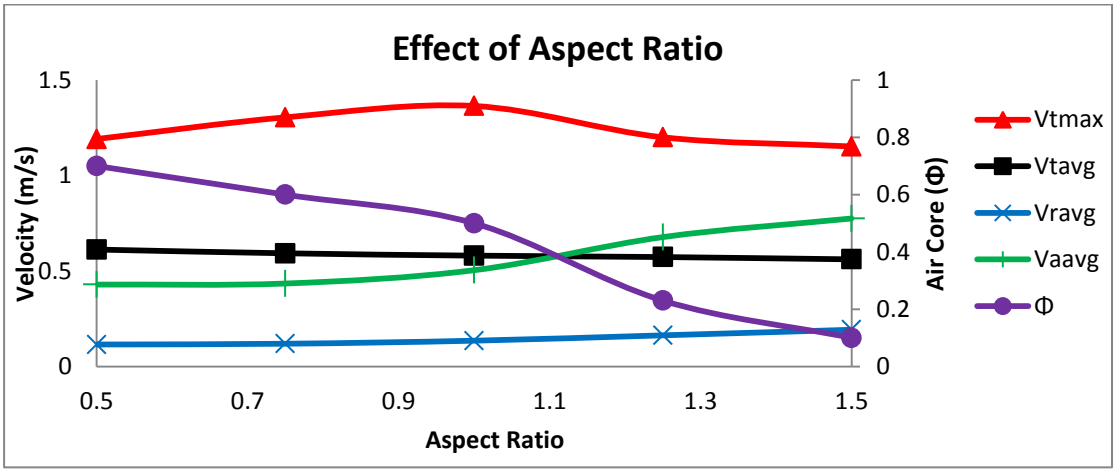

Figure 3. 5 Effect of Basin Height on air-core and Tangential, Radial and Axial Velocity

3.1.3 EFFECT OF BASIN DIAMETER

Increasing the basin diameter from a minimum value causes the water height to reduce. Although this causes an approach towards conditions of critical submergence and ultimately towards the formation of an air-core vortex. But this approach towards formation of an air-core formation only increases till a particular value of basin diameter after that value, the friction offered by the basin floor increases and causes a reduction in the tangential velocity. This decerease in tangential velocity causes a decrease in the air core. Moreover, the water tends to move radially inwards instead of tangential motion. This is due to the increased friction in tangential movement due to increase in the friction offering basin floor area.

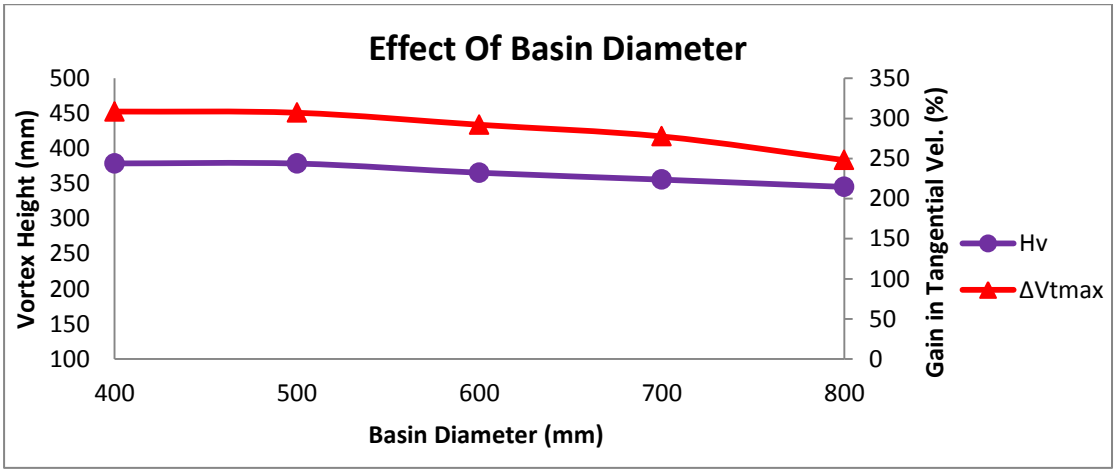

Figure 3. 6 Effect of Basin Diameter on Vortex height and gain in tangential velocity

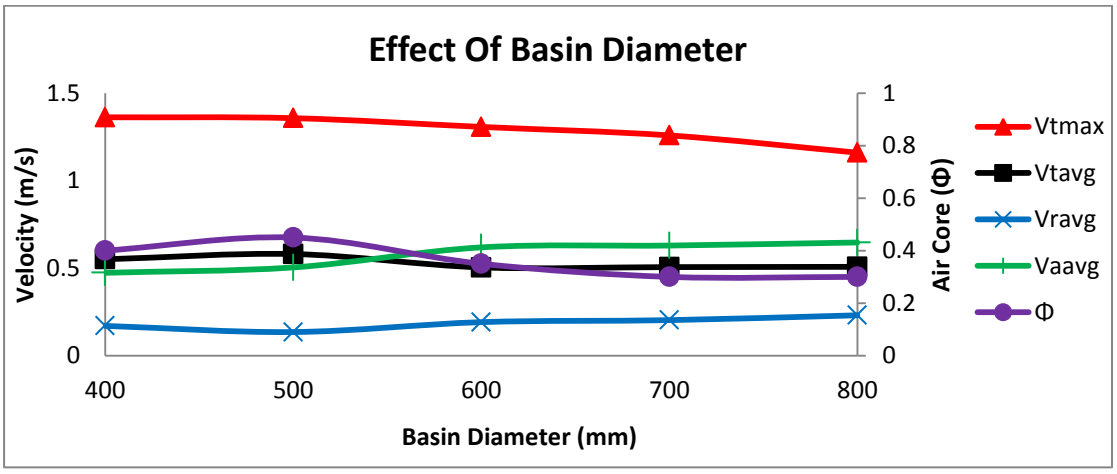

Figure 3. 7 Effect of Basin Diameter on Air-core and Tangential, Radial and Axial Velocity

3.1.4 EFFECT OF OUTLET DIAMETER

The effect of outlet diameter is observed in the form of ratio of outlet diameter to the basin diameter. Increasing this ratio allows more water to flow out of the basin outlet, therefore a reduction in the water height in the basin is observed. When the submergence of the outlet is lesser than the critical submergence, air-core is formed. Since the critical submergence increases by increasing the outlet diameter, while the water level decreases, this causes a tendency towards air-core formation. The decrease in vortex height causes the tangential velocity to decrease negligibly. Therefore the tangential velocity appears to be almost constant. The maximum tangential velocity also decreases negligibly due to the decrease in vortex height. When the water height reduces, the friction offered by the basin floor is more significant. The decrease in axial velocity is a result of the reduced water height in the basin.

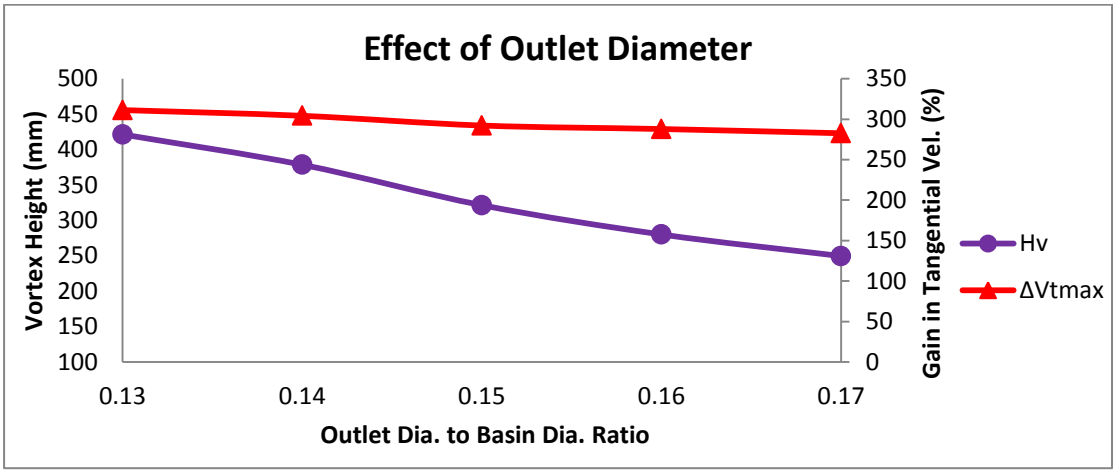

Figure 3. 8 Effect Of Outlet Diameter On Vortex Height And Gain In Tangential Velocity

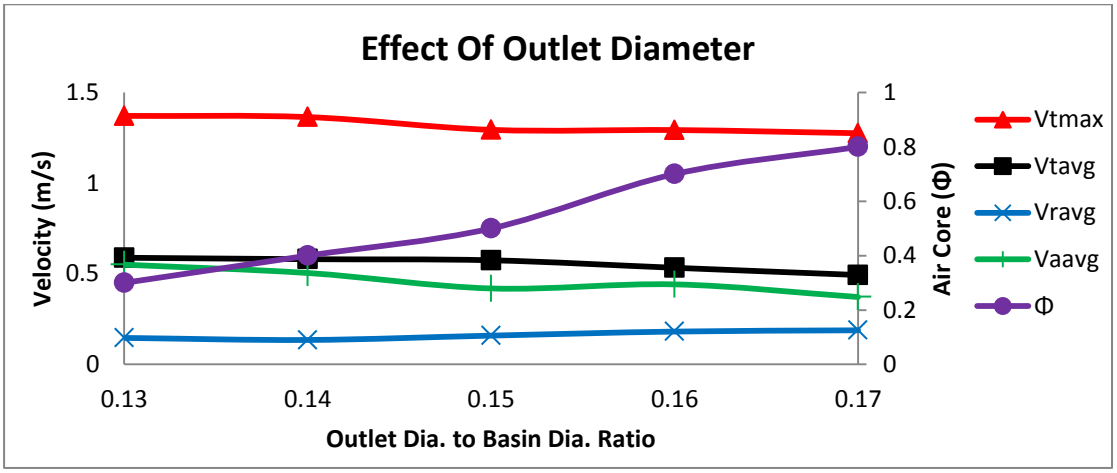

Figure 3. 9 Effect of Outlet Diameter on Air-core and Tangential, Radial and Axial Velocity.

3.1.5 EFFECT OF INLET WIDTH

The effect of inlet width is observed with respect to the basin diameter. The analysis shows that the optimum ratio of inlet width to the basin diameter lies in the range of 0.2 to 0.3. An increase in this ratio increases the mass flow into the basin, which causes the water height to rise till overflow from the upper walls of the basin occurs. the air core diminishes since the excessive mass of water that enters the basin replaces the air core. the axial velocity at the vortex core increases due to the increased water height in the basin, while the tangential velocity decreases due to the reduction in air core. The reduction in tangential velocity is caused by the turbulent entry of the water into the basin due to the wider inlet channel as compared to the basin diameter. The distortion of air core also results in an increase of radial velocity.

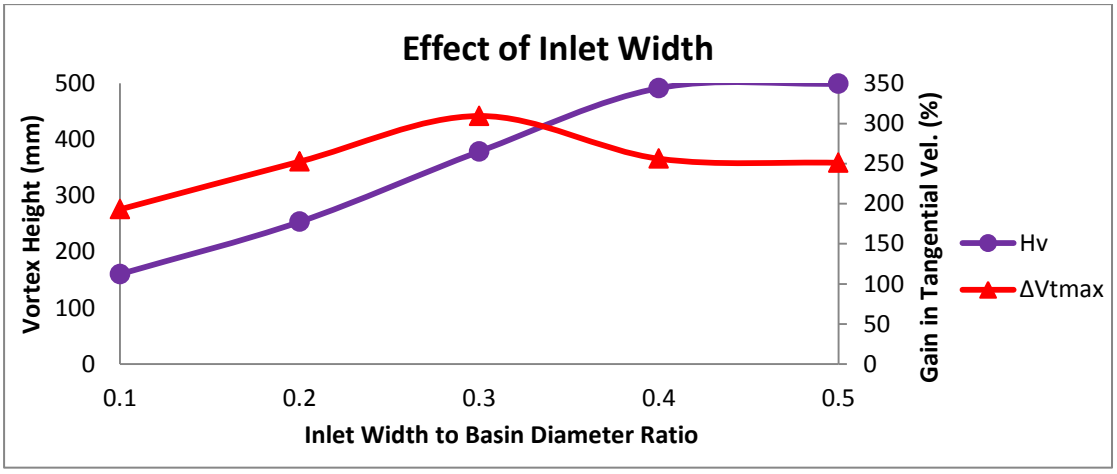

Figure 3. 10 Effect Of Inlet Width On Vortex Height And Gain In Tangential Velocity

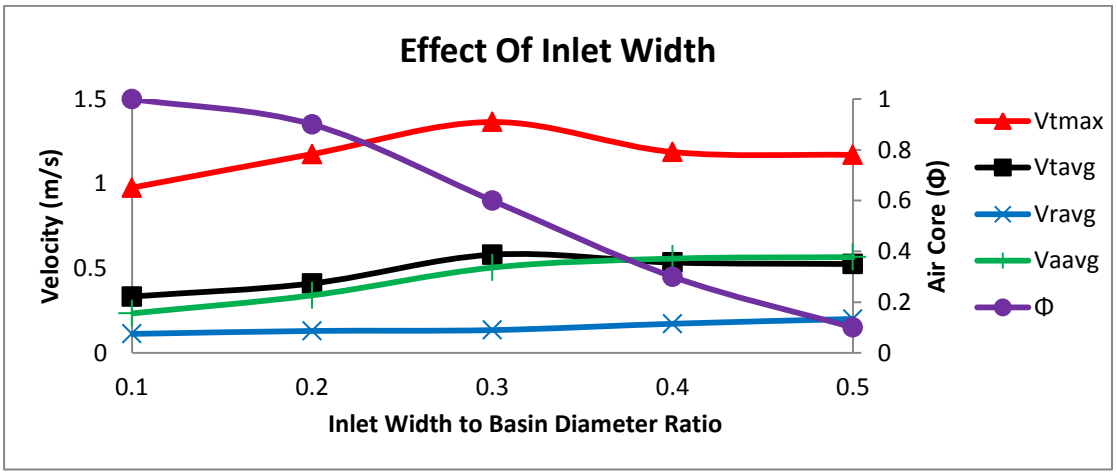

Figure 3. 11 Effect of Inlet Width on Air-core and Tangential, Radial and Axial Velocity

3.1.6 EFFECT OF INLET DEPTH

An increase in inlet depth increases the mass flow into the basin, which causes the water height to rise till overflow from the upper walls of the basin occurs. The effect of inlet depth is plotted in terms of ratio of inlet depth to basin height. An increase of this ratio causes the air core to diminish since the excessive mass of water that enters the basin replaces the air core. The axial velocity at the vortex core increases due to the increased water height in the basin, while the tangential velocity decreases due to the reduction in air core. But the tangential velocity and air core formed in this case is higher than that achieved when increasing the inlet width. This is due to the smoother entry of water into the basin. When water enters at a distance, through a narrow inlet, the vortex distortion is lesser as compared to that observed in case of increase in inlet width. This also causes an increase in the tangential velocity.

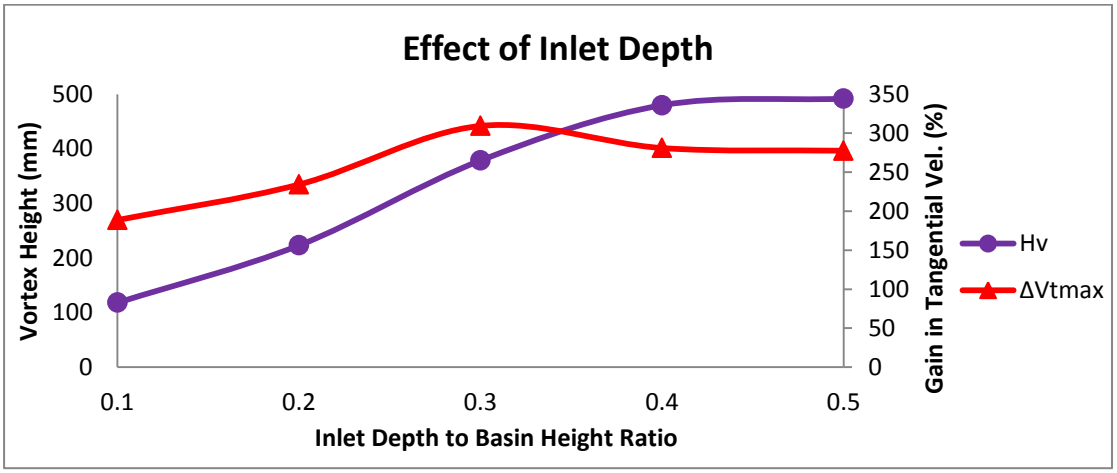

Figure 3. 12 Effect of Inlet Depth on Vortex height and gain in tangential velocity

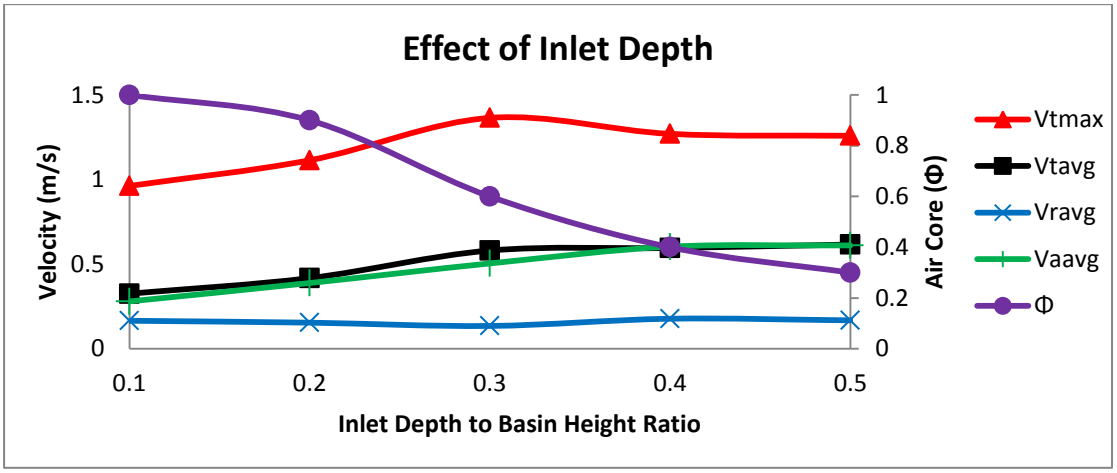

Figure 3. 13 Effect of Inlet Depth on Air-core and Tangential, Radial and Axial Velocity

3.1.7 VORTEX FORMATION IN OPTIMIZED BASIN

The optimized basin generates a full-air core vortex which is far more suitable for power generation using a mass flow rate of 4.5 kg/s. The basin was optimized by narrowing of the inlet channel so as to smoothen the entry of water into the basin, increasing the height of the inlet channel to allow the formation of a vortex with higher height and by increasing the size of the bottom outlet. The combined effects of these modifications led to the fomarion of a full air-core with a higher vortex height. Moreover, the optimized basin resulted in 85.5% increase in in the tangential velocity as compared to the initial/reference basin. This increase in the tangential velocity is due to the formation of air core. Figure 3. 14 (a) shows the streamlines and the water-air interface in the optimized basin and the vortex formed. The vortex formed in this basin is fully developed and extends from the top of water surface down to the bottom outlet of the basin. Figure 3. 14(b) shows the separation between air and water in the form of volume fractions of air and water. The upper blue region indicates the air, while the lower red region indicates the water present inside the basin.

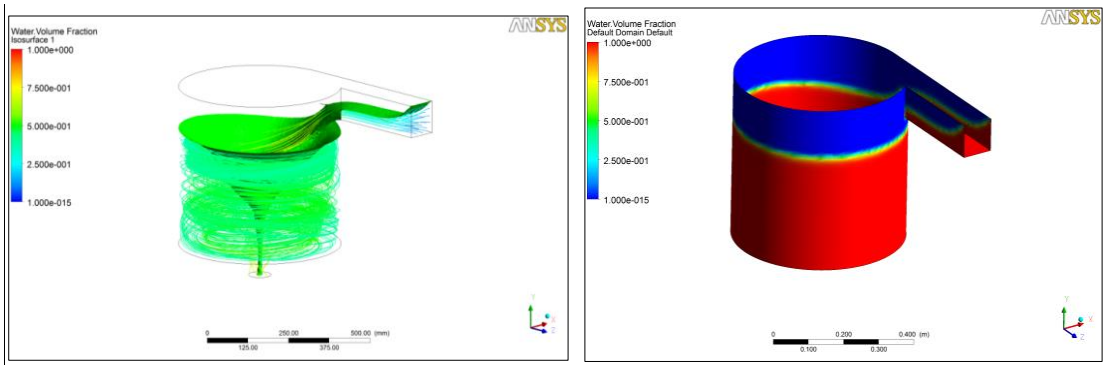

(a) (b)

Figure 3. 14 Velocity streamlines and vortex formed in the optimized basin

3.2 RESULTS OF BLADE ANALYSIS

The insertion of blades in the basin causes a distortion in the fluid flow. This disturbance causes a decrease in the height of the vortex due to the decrease in the tangential velocity of the fluid and a corresponding increase in the radial and axial velocities. Figure 3. 15 (a) shows how the blade domain is inserted in the basin domain. Figure 3. 15 (b) shows the vortex formation in the presence of the blades and the water and air regions in the basin. Figure 3. 15 (c) shows the decrease in vortex height when the blades in the basin are rotating at 50 rpm and Figure 3. 15 (d) shows the velocity streamlines formed in the presence of blades.

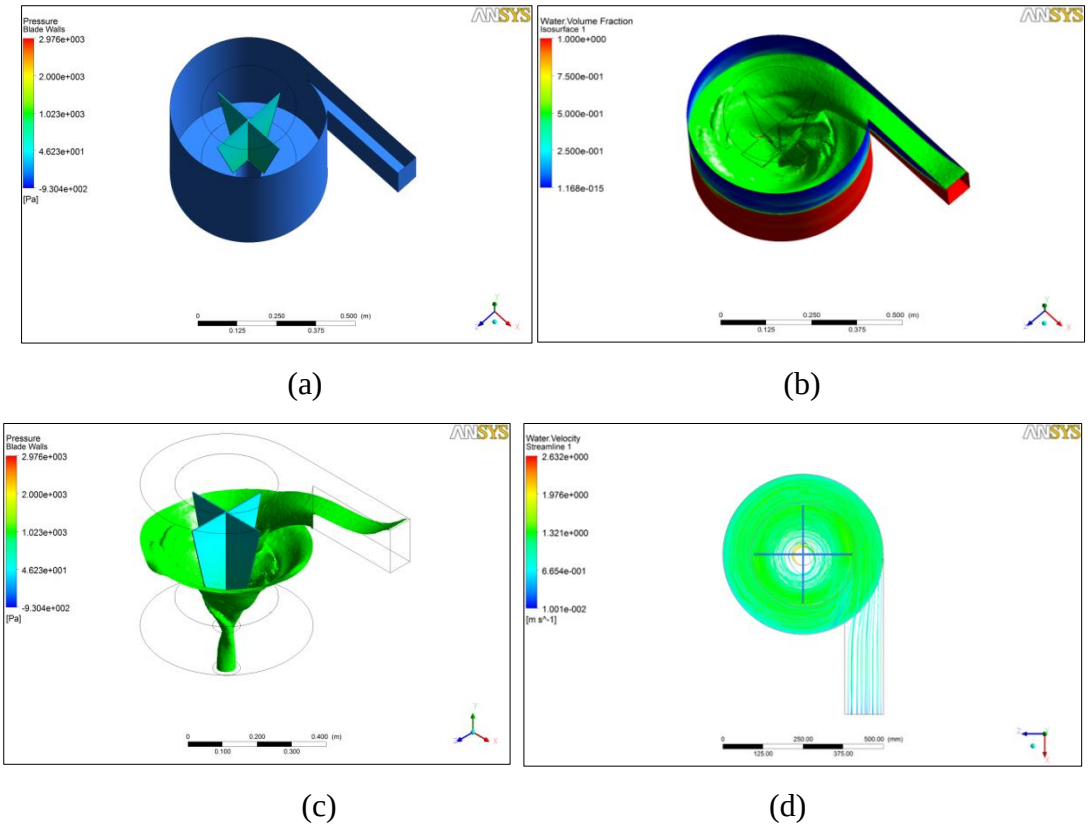

(a) (b)

(c) (d)

Figure 3. 15 Velocity streamlines and vortex formation in the optimized basin in the presence of rotating blades

3.2.1 EFFECT OF RPM ON TORQUES

Torques are applied on the blades when the blades are placed in the path of fluid flow. Decreasing the angular velocity of the blades causes an increase in the torques obtained at blades. The non-linear behavior of the graphs shown in Figure 3.15 is due to variation of the vortex height, caused by the blades at different angular velocities. The torques on cross flow blades are more than that on any other blade. This is due to the shape of the cross flow blades, which causes a lesser distortion in the vortex profile and extracts maximum kinetic energy of the flowing water. The torque on curved blades is the least at all rpms because the curved blades allow water striking them to smoothly pass over their surface and to move towards the center of the vortex core, thereby distorting the vortex more than any other blade and therefore the torques on curved blades are lesser. The twisted blades yield higher torques than the conical blades, since their contact area is more as compared to the conical blades.

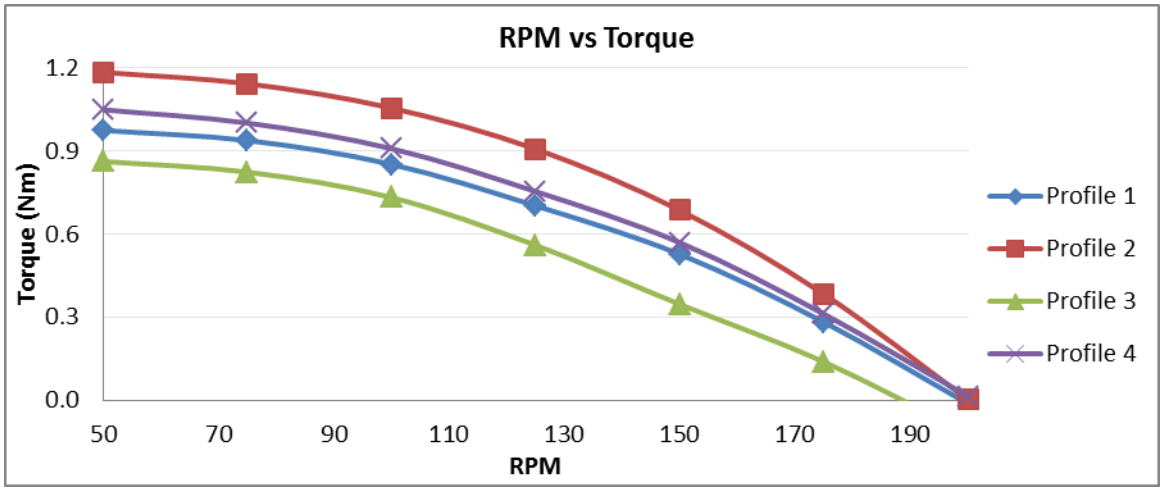

Figure 3. 16 Effect of RPM on torques generated at blades

3.2.2 EFFECT OF RPM ON VORTEX HEIGHT

With no blades installed inside the vortex, the water flows in tangential direction and results in a particular height of the vortex. The placement of blade distorts the vortex profile and increases the radial and axial components of velocity while decreasing the tangential components. This decrease in tangential velocity causes a decrease in the height of vortex. As the angular velocity of the blades is increased, the distortion in the vortex profile decreases and the tangential velocity of the water increases. Thus higher angular velocities result in a higher vortex height in comparison to lower angular velocities. Different blades distort the vortex to a different value and therefore decreasing its height, depending upon how the fluid flows in the presence of these blades. The cross flow blades cause a minimum distortion to the vortex due to the shape of the blades, which does not allow the striking water to move towards the center of the air core, rather it keeps the water flowing along the vortex profile. Similar vortex height is observed when the conical blades are analyzed, since the conical blades are along the vortex profile. The decrease in vortex height caused by curved blades is more than any other blade due to its curved shape which directs the water towards the center of air core after striking it and thus causing a reduction in the vortex height. Although the twisted blades are not along the shape of the vortex profile, but these blades also keep the water flowing along the free vortex path and thus resulting in higher vortex height as compared to the curved blades.

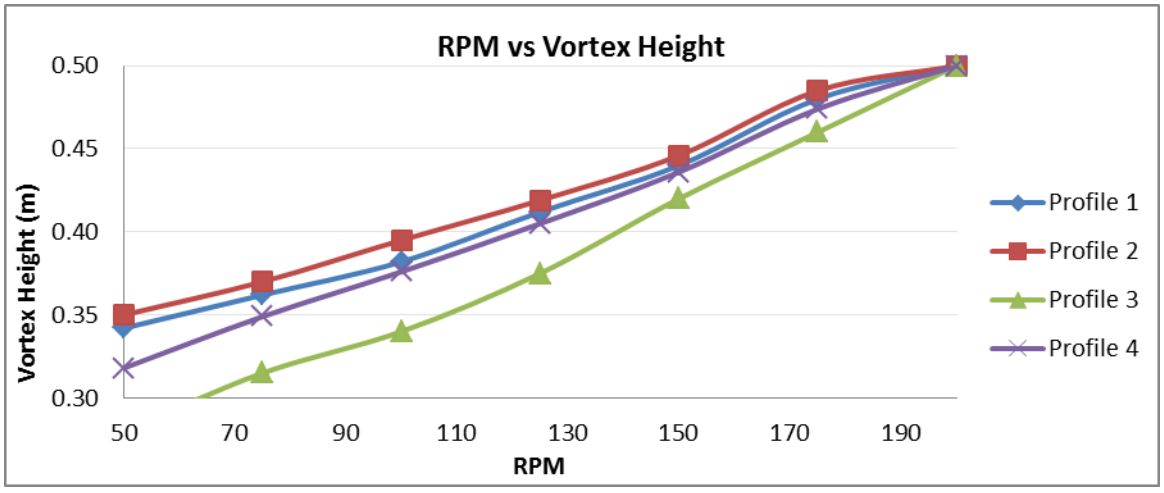

Figure 3. 17 Effect of RPM on the vortex height

3.2.3 EFFECT OF RPM ON EFFICIENCY

Best efficiency is obtained at almost mid rpms between the maximum load condition and no load condition for all blades. The values of efficiencies for cross flow blades are higher as compared to other blades, since the torques generated on these blades are maximum. The higher efficiency of the cross flow blades may be attributed to the vortex retaining capability of the blades which ultimately result in higher torques. The curved blades are less efficient due to their shape which poorly extracts energy from the vortex and cause a considerable reduction in the vortex height. Conical blades yield a maximum efficiency of 44.65% at 125 rpm. Cross flow blades yield a maximum efficiency of 57.69% at 125 rpm. Curved blades yield a maximum efficiency of 37.25 % at 100 rpm. Twisted blades yield a maximum efficiency of 47.95% at 125 rpm.

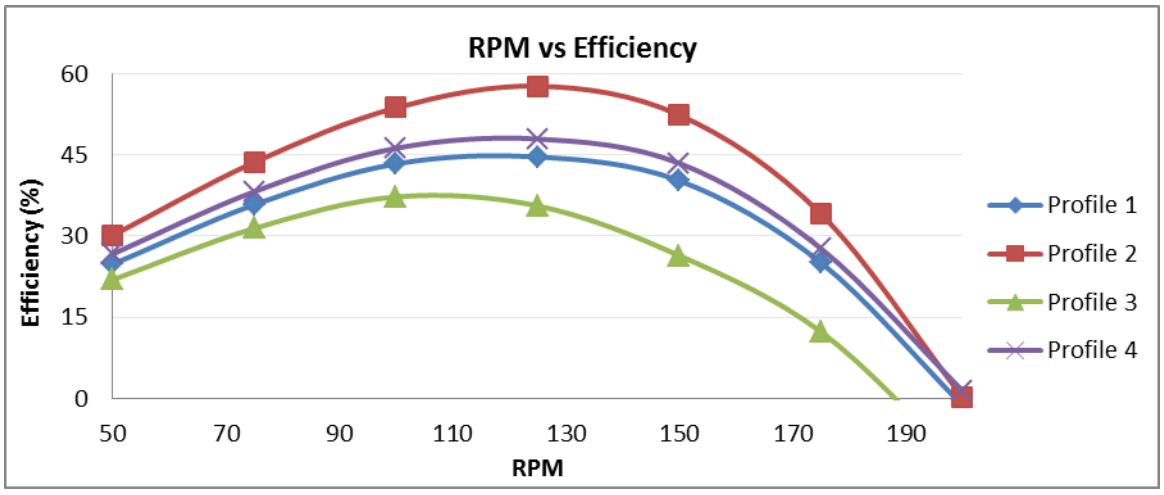

Figure 3. 18 RPM versus efficiency curve

As illustrated in Article 3.1.2, Figure 3. 4 and Figure 3. 5, the height of water inlet above the vortex surface does not affect the vortex formation. This makes the height of the vortex as the head of the water. Therefore efficiency can also be plotted in terms of the vortex height rather than the total head of the inlet channel. When the efficiencies of the four blades with respect to the vortex height are plotted against rpms, it was found that the cross flow blades still yield the maximum efficiencies. Conical blades yield a maximum efficiency of 56.74% at 100 rpm, cross flow blades yield a maximum efficiency of 68.84% at 125 rpm, curved blades yield a maximum efficiency of 54.78 % at 100 rpm while twisted blades yield a maximum efficiency of 61.49 % at 125 rpm. Moreover, at lower rpms, the curved blades yield better efficiencies than conical blades.

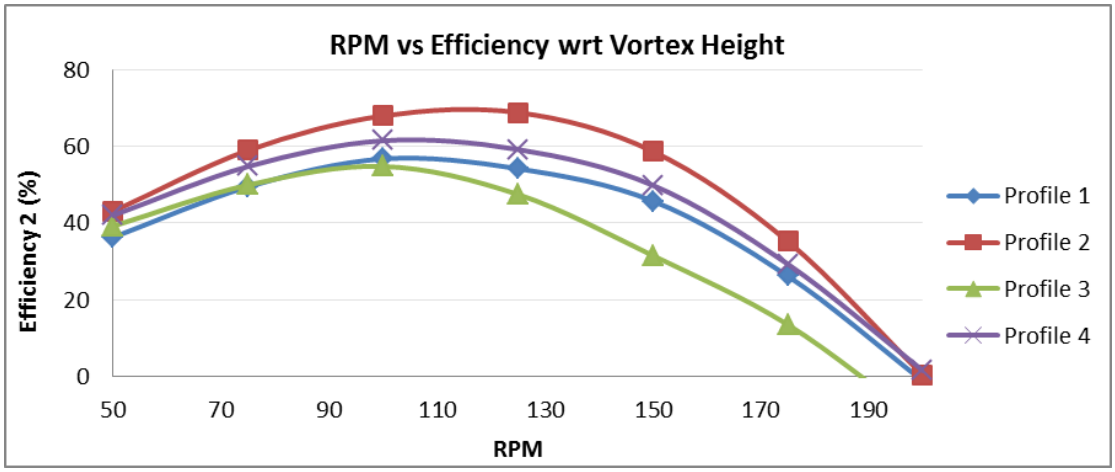

Figure 3. 19 RPM versus efficiency w.r.t vortex height

CHAPTER 4. EXPERIMENTS

For the experimental validation of the numerical results, an experimental setup was fabricated, which was used to check the validity of the numerical results and to test the vortex formation. The model was later optimized using the results obtained from CFX. The optimized model was then tested for the power generation in the form of a GWVPP.

4.1 EXPERIMENTAL SETUP

The dimensions of the laboratory model were based on the available literature and then the setup was modified based on the findings of numerical analyses so as to form a strong air core vortex, for the production of mechanical power. In case of the prototype, the circulation required for the generation of the vortex is achieved by the tangential entry of water into the cylindrical basin. A schematic of the experimental setup is shown in Figure 4. 1. A pump provides water to the inlet channel which directs it into the vortex pool. After the formation of vortex, the water exits through the bottom hole of the basin and moves into the water reservoir, from where it is recirculated by the pump. The flow rate is controlled by the ball valve which is installed in the loop after the pump.

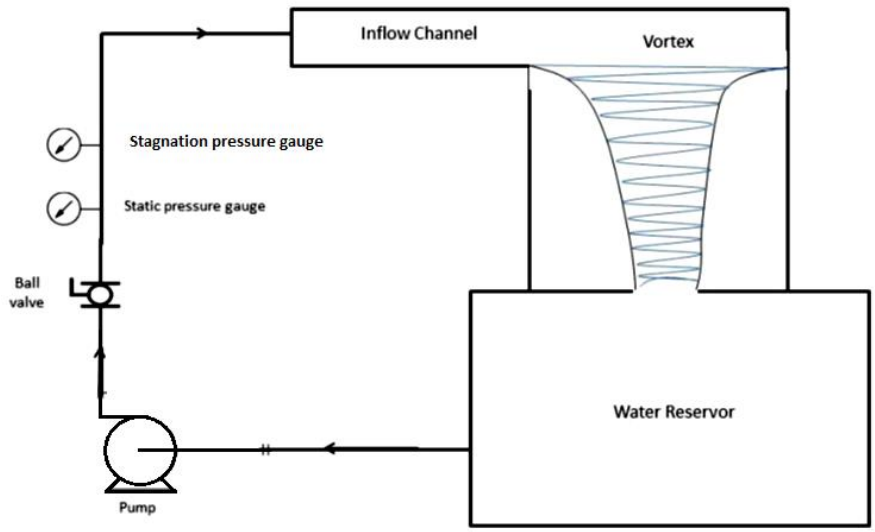

Figure 4. 1 Schematic of Experimental Setup

4.2 BASIN FABRICATION

Galvanized iron sheets were used for the fabrication of the basin wall. The dimensions of the reference basin and the optimized basin are given in Table 2.1 and Table 2.3. The experimental model of the basin is shown in Figure 4. 2 (a). A plate of the same

material was used at the inlet to enable the inlet width to be changed according to the optimized design of the basin. Discs having holes of different diameters were used to enable the modification of the outlet diameter of the basin for optimization. These discs were placed at the bottom of the basin, which would ultimately change the outlet diameter. Based upon the findings of ANSYS CFX, the dimensions of the optimized basin are used for the basin model. The height of the basin is 500mm and the diameter of the basin is also 500mm. The inlet channel is at the top and has a width and depth of 100mm each. The diameter of the oulet is 80mm.

4.3 BLADES FABRICATION

All of the blades were made of steel sheets of 2 mm. The dimensions of the blades are shown in Appendix A. The selection of the dimensions is already discussed in Section 2.3.1

(a) Basin

(b) Blades

(c) Reservoir

(d) Pump

Figure 4. 2 Various Components of Experimental Setup

4.3.1 BLADE SUBMERGENCE CONTROL

The blade height was controlled by using a shaft of length that extends from top of the basin to the drain hole at the bottom. The diameter of the shaft is 12.7 mm and is made of steel. The length of this shaft is 500mm so as to enable the placement of blade at any height along the vortex. The position of the blades was fixed by using bolts that would help different blades to be fixed at different positions along the shaft.

The assembly of all the components of the experimental setup along with few auxillaries is shown in Figure 4. 3

Figure 4. 3 Experimental Setup

4.4 AUXILLARIES

Various other components that were required for the development of the experimental setup are:

4.4.1.1 TOP FRAME

A frame of acrylic sheet was used to hold the blades firmly in their position along the axis of the vortex core. Two bearings were fixed in the top frame to allow a frictionless contact.

4.4.1.2 PUMP

A pump was used for the supply of water into the basin inlet. The pump is a centrifugal pump which has a maximum discharge capacity of 500 liters /min.

4.4.1.3 PIPING

Galvanized iron pipes of 2" diameter were used for the supply of water from the pump to the inlet of the basin. A ball valve was used to control the flow rate.

4.4.1.4 WATER RESERVOIR

A water reservoir was used to make a closed loop of water flow so as to avoid water wastage. The reservoir stores the water that flows out of the basin drain hole and supplies it to the pump for reuse at the basin inlet. The water reservoir was domestic water tank made of fiber glass and had a capacity of 0.568 m^3 (150 Gallons).

4.5 MEASUREMENT DEVICES

i. Pressure gauges for flow rate measurement:
ii. Prony brake for torque measurement:
iii. Digital tachometer for rpm measurement

4.6 EXPERIMENTAL PROCEDURE

Flow rate was measured by calculating the dynamic pressure by the help of two pressure gauges. One of these gauges measured the static pressure while other measured the stagnation pressure. The difference of the two gauge readings gives the dynamic pressure. The dynamic pressure was used to calculate the velocity of the water, which was further multiplied by the area of the pipe to get the volumetric flow rate. The flow rate, Q, was maintained at 4.2 liters / second.

A domestic bucket of 30 cm height and 35 cm diameter was graduated at 22 liters to cross check the calculated volumetric flow rate through the pump. The time which was taken by the pump to fill the bucket was measured using a stop watch.

$$P_{dynamic} = P_{stagnation} - P_{static} \quad (1)$$

$$Velocity = v = \sqrt{\frac{2\,P_{dynamic}}{\rho}} \quad (2)$$

$$Flow\ rate = Q = Av \quad (3)$$

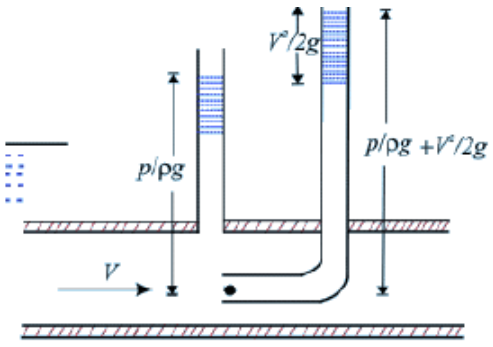

Figure 4. 4 Velocity measurement

The basin was graduated at different levels to measure the height of the vortex. A coupler was attached to the top of the output shaft (shaft connected to the blades). The radius of the coupler was 19 mm. Spring balances were used to apply force to the output shaft. This force measured by the spring balances, when multiplied by the radius of the coupler gives the torque applied on the shaft. A digital tachometer was used to measure the angular velocity of the output shaft.

$$Torque = \tau = rF \quad (4)$$

$$Input\ Power\ 1 = \rho g \mathrm{H} Q \quad (5)$$

$$Input\ Power\ 2 = \rho g \mathrm{h_v} Q \quad (6)$$

$$Output\ power = T\omega \quad (7)$$

Efficiency, which is the ratio of output power to input power was determined as:

$$Efficiency = Output\ Power / Input\ Power \quad (12)$$

$$Efficiency\ 2 = Output\ Power / Input\ Power\ 2 \quad (13)$$

4.7 EXPERIMENTAL RESULTS

4.7.1 EFFECT OF TORQUE ON ANGULAR VELOCITY

The angular velocity of the blades decreases when the force applied on the blades is increased. This decrease becomes drastic when the torques are increased significantly. The sudden decrease is angular velocity is due to the decrease in vortex height, which implies the decrease in vortex strength. The decrease in vortex strength causes a decrease in the angular velocity of the blades. This is shown in Figure 4. 5

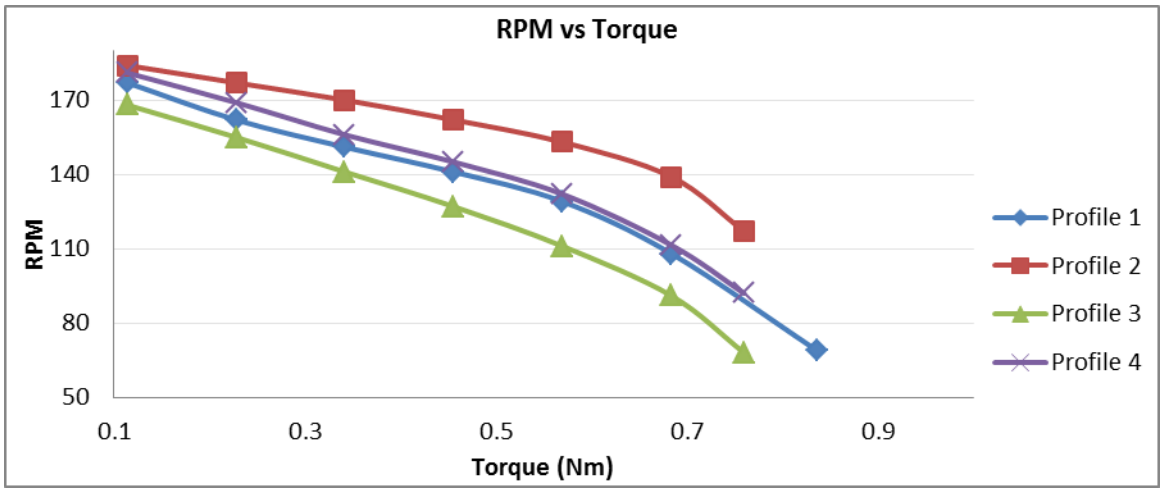

Figure 4. 5 Effect of torque on angular velocity of blades

4.7.2 EFFECT OF TORQUE ON VORTEX HEIGHT

The increase in torques applied on the blades causes a decrease in angular velocity which correspondingly decreases the vortex height as shown in Figure 4. 6. The decrease in vortex height due to cross flow blades is minimum because the cross flow blades keep the water moving along the vortex flow direction, while the decrease in vortex height is maximum in case of the curved blades because the curved blades change the direction of the water striking the blade edges from tangential to radial.

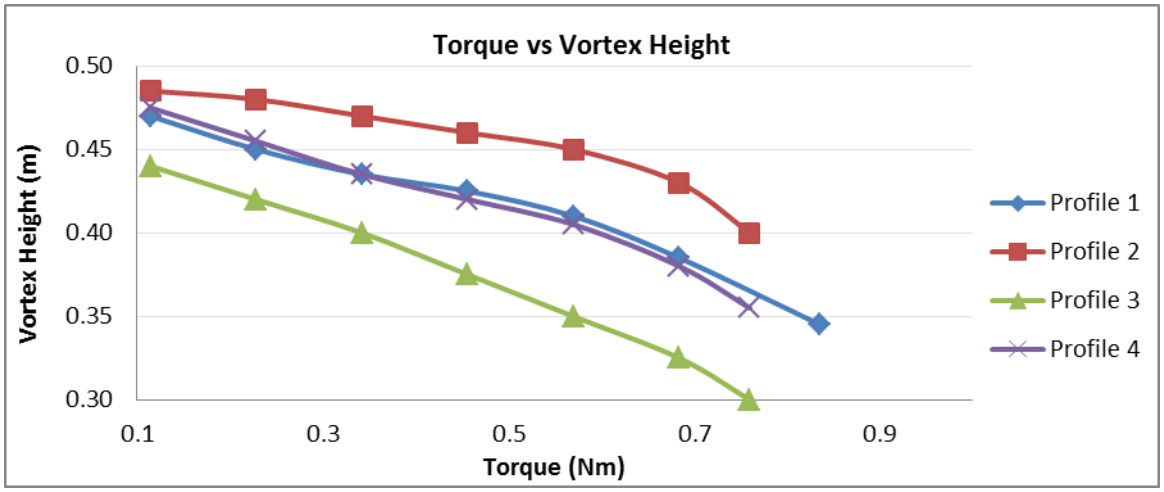

Figure 4. 6 Effect of torque on Vortex Height

4.7.3 TORQUE VERSUS EFFICIENCY

Increasing the resisting torque on the coupler causes an increase in the load on the turbine. When the load on the turbine is increased, the angular velocity of the blades decreases. This causes a change in the efficiency of the plant. The efficiency increases till the vortex distorts significantly due to the disturbance in the flow. The optimum torque at which highest efficiency is obtained, lies half way between no force on the blade and the maximum force to stop the blade as shown in Figure 4. 7.

i. Conical blades (Profile 1) yield a maximum efficiency of 37.59% at 108 rpm.

ii. Cross flow blades (Profile 2) yield a maximum efficiency of 48.38% at 139 rpm.

iii. Curved blades (Profile 3) yield a maximum efficiency of 32.20 % at 112 rpm.

iv. Twisted blades (Profile 4) yield a maximum efficiency of 38.78% at 111 rpm.

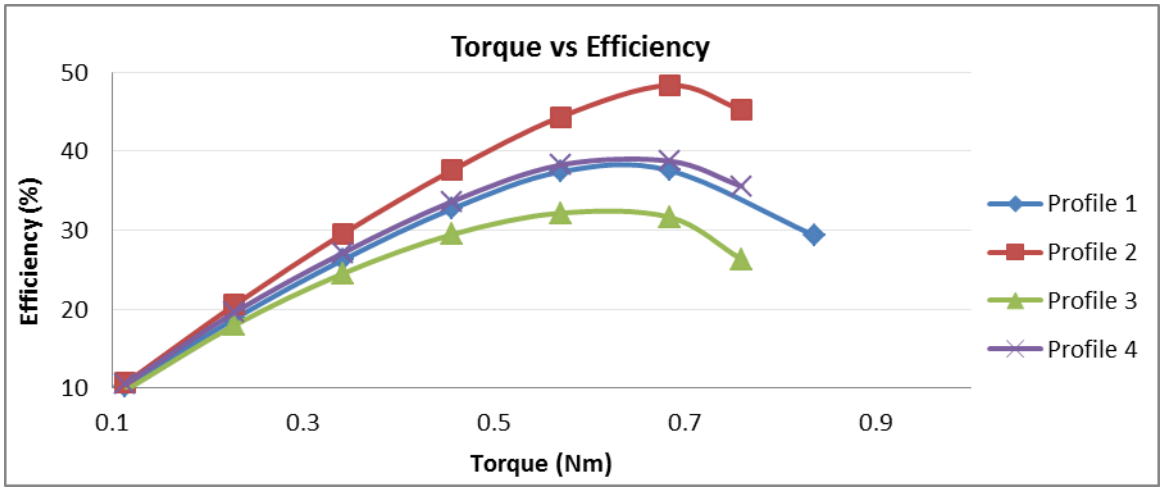

Figure 4. 7 Torque versus Efficiency Curve

When the efficiency of blades is plotted using the vortex height as the total head, the cross flow blades are found to be more efficient as compared to other blades. The difference between the efficiencies is more clear when higher resisting torques are applied on the blades. Conical blades yield a maximum efficiency of 48.82% at 108 rpm, cross flow blades yield 56.56 % at 117 rpm, curved blades yield 48.73 % at 91 rpm while twisted blades yield a maximum efficiency of 51.03 % at 111 rpm.

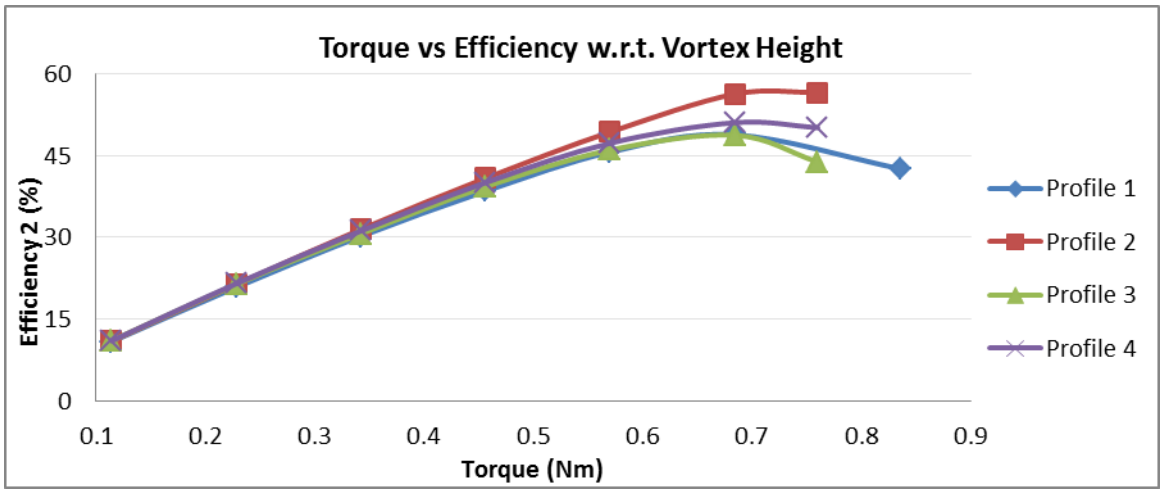

Figure 4. 8 Torque versus Efficiency w.r.t. Vortex Height

4.8 COMPARISON OF RESULTS

The results obtained from CFX simulations showed close resemblance with those obtained experimentally while an error ranging from 6 to 15% was observed in different cases. Figure 4. 9 indicates the difference observed between numerical and simulational results for one of the blades. Since frictional forces are not considered in the numerical analysis, therefore the power obtained numerically is slightly higher

than the power obtained experimentally. Moreover, at higher rpms, the centrifugal forces cause an increase in the height of vortex, which result in higher torques on the blades. A similar trend is observed for all the blades, as shown in Figure 4. 10.

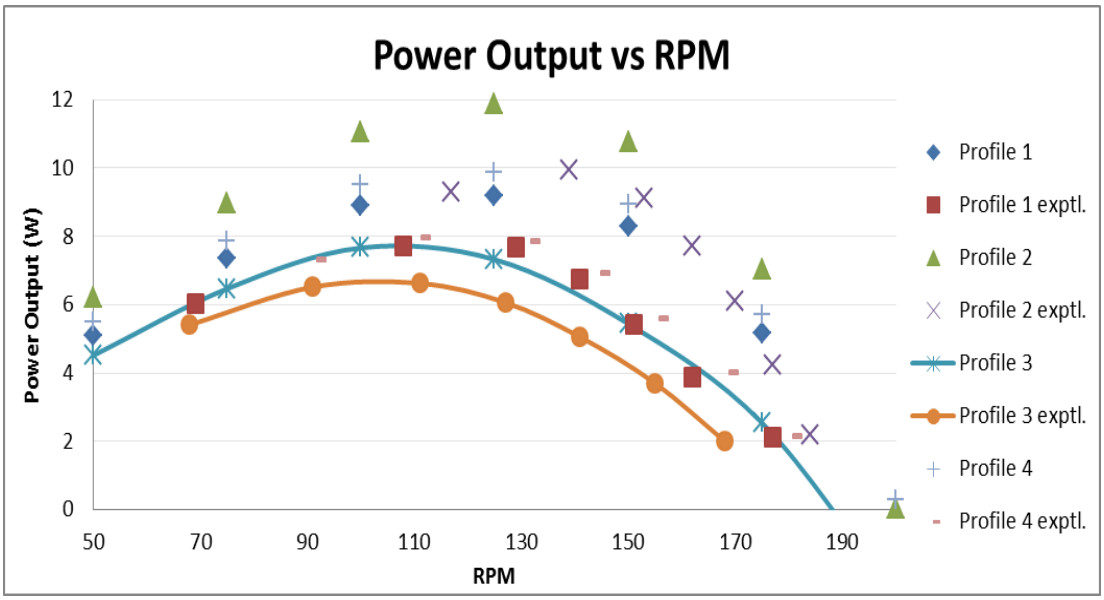

Figure 4. 9 Comparison of Numerical and Experimental Output Power

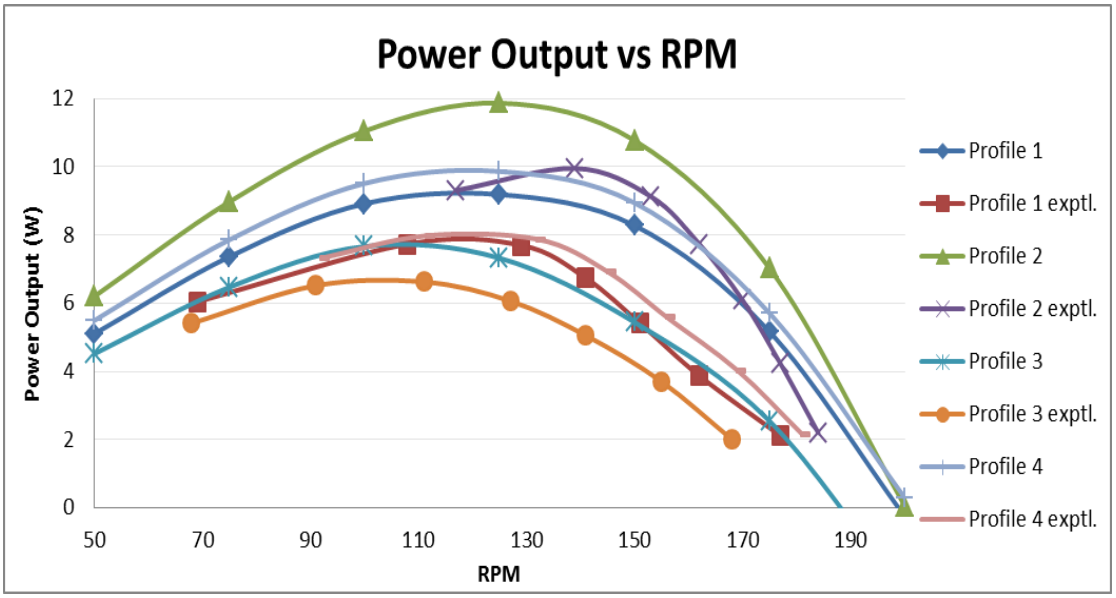

Figure 4. 10 Comparison of Numerical and Experimental Output Power for all Blades

The difference between the numerical and experimental results increases at higher angular velocities. This is due to the methodology used for numerical analysis of the blade. In simulations, the blade rotation is an input parameter. At higher angular velocities, the centrifugal forces come into play and the blades tend to cause an outward flow of the water which causes a reduction in the radial velocity and thereby

increasing the vortex height as shown in Figure 4. 11. Similar trend is observed for all the blade profiles as shown in Figure 4. 12.

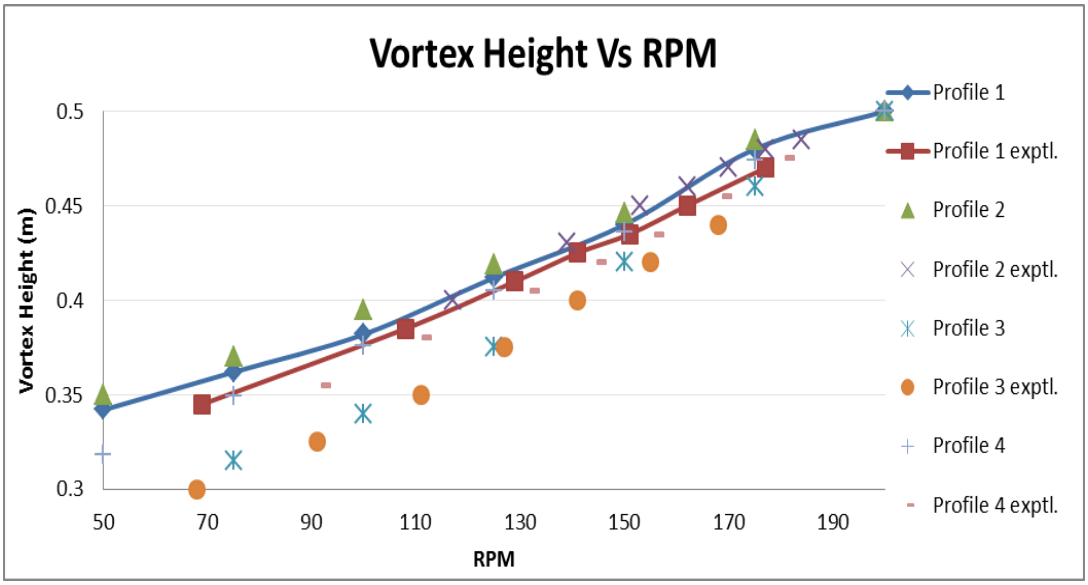

Figure 4. 11 Comparison of Numerical and Experimental Vortex Heights

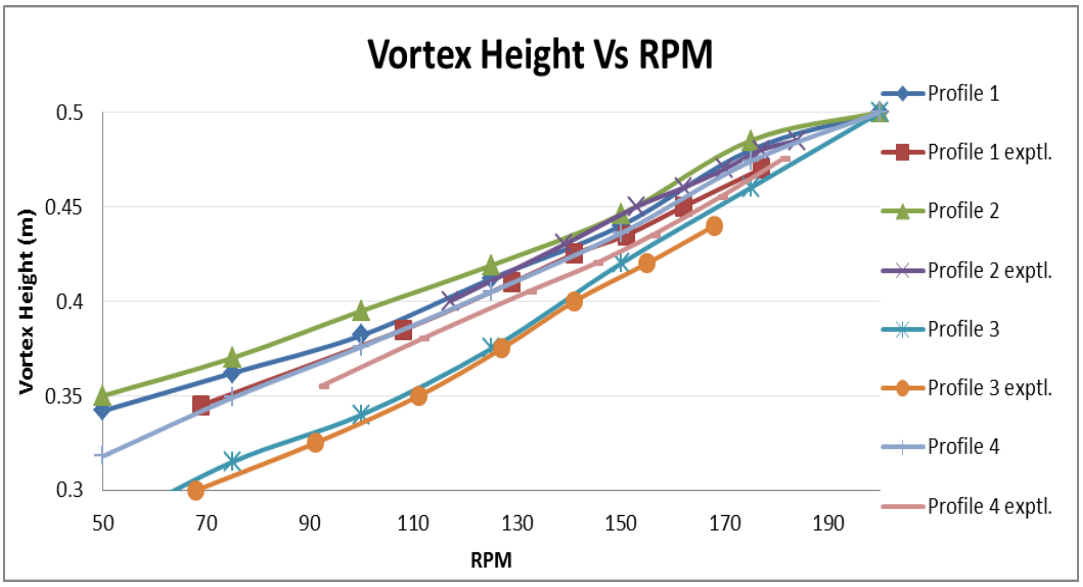

Figure 4. 12 Comparison of Numerical and Exp. Vortex Heights for all Blades

The difference between numerical and experimental results of efficiency for all the blades at their best efficiency points are shown in Table 4. 1

Table 4. 1 Difference between Numerical and Experimental Efficiencies

Blade	Diff. between Numerical and Exp. Results	
	Efficiency 1	Efficiency 2
Profile 1	7.06	7.92
Profile 2	9.31	12.28
Profile 3	5.05	6.05
Profile 4	9.17	10.46

CHAPTER 5. CONCLUSIONS

The GWVPP is an efficient power plant that can be used to generate power easily using a low head. Based on the findings of the research, it can be concluded that:

i. RNG k-ε Turbulence Model can be used for the case when parametric study is done in the absence of blades. This model requires lesser computational time as compared to SST Turbulence Model.
ii. SST Turbulence Model predicts the torques and vortex heights almost accurately.
iii. An increase of flow velocity or mass flow rate into the basin causes a rise in the height of water level with an increase in the tangential velocity
iv. The velocity increase in the vortex is maximum when a full air core is formed.
v. The air core and vortex height cannot be directly related to each other since the air-core formation depends upon many other factors as well.
vi. Increasing the flow rate by increasing the inlet depth is a better option as compared to the inlet width.
vii. Air core can be formed by increasing the outlet diameter keeping all other parameters constant.
viii. When the basin diameter is reduced, the water level in the basin slightly increases. But the reduction of basin diameter causes the air core to decrease till the air-core eventually dies.
ix. As the basin diameter is increased from the optimum value, the vortex height decreases, and thus the strength of the vortex.
x. When a basin of larger diameter is used, the vortex height drops and almost all the water glides along the floor of the basin. This causes a great frictional loss in the velocity of the water.
xi. Water entry above the vortex upper surface does not result in any positive output.
xii. Optimum torque lies in the mid of the whole rpm range i.e. between no load condition and maximum load condition. Best efficiency point also lies in the mid of the rpm range.
xiii. Heavier blades result in lower rpms.
xiv. Blades of profile 2 are concluded to be more efficient as compared to other blade profiles since they are able to harness more power.

xv. The difference between the experimental and numerical results increases as the blade weight increases.

xvi. When the load on the turbine is increased, it decreases the height of the vortex.

FUTURE RECOMMENDATIONS:

1. Installation of guide vanes
2. Further optimization of Cross flow and twisted blades
3. Testing of the proposed blade profiles in different basin geometries
4. Using a better quality mesh for the improvement of results.

REFERENCES

[1] M Lapuerta, O Armas, and J R Fernandes, "Effect of biodiesel fuels on diesel engine emissions," *Progress in Energy and Combustion Science*, vol. 34, pp. 198-223, 2008.

[2] B S Chauhan, N Kumar, and M C Haeng, "A Study on the Performance and Emission of a diesel engine fuelled with Jatropha biodiesel oil and its blends," *Energy*, vol. 37, pp. 616-622, 2012.

[3] (2015) What is Renewable Energy? [Online]. http://extension.psu.edu/natural-resources/energy/

[4] Ziy Wang, Qinxing Wang, Ronald Wennersten, and Qie Sun, "Transitions to sustainable energy and material systems –," *Energy Procedia*, vol. 75, pp. 2083-2093, 2015.

[5] Bruce R Munson, H Theodre Okiishi, and W Wade Huebsch, *Fundamentals of Fluid Mechanics*, 6th ed.

[6] ME Mechanical Team. (2016, April) Comparison of Impulse and Reaction Turbines. [Online]. http://me-mechanicalengineering.com/comparison-between-impulse-turbine-and-reaction-turbine/

[7] O B Yaakob, M Ahmed Yasser, A H Elbatran, and H M Shabara, "A Review on Micro Hydro Gravitational Vortex Power and Turbine Systems," *Jurnal Teknology*, vol. 69, no. 7, pp. 1-7, 2014.

[8] S Sivanagaraju, M B Reddy, and D. Srilatha, *Generation and Utilization of Electrical Energy*. India: Pearson Education, 2010.

[9] Aravind Venukumar, "Artificial Vortex (ArVo) Power Generation- An Innovative Micro Hydroelectric Power Generation Scheme," in *Global Humanitarian Technology Conference: South Asia Satellite (GHTC-SAS) IEEE 53-57*, 2013.

[10] How to plan a Micro-hydro Power Plant. [Online]. http://en.howtopedia.org/wiki/How_to_Plan_a_Micro_Hydro-power_Plant

[11] A H Elbatran, H M Shabara, O B Yaakob, and M Ahmed Yasser, "Operation, Performance and Economic Analysis of Low Head Micro-Hydropower Turbines for Rural and Remote Areas: A Review," *Renewable and Sustainable Energy Reviews*, vol. 43, pp. 40-50, 2015.

[12] Han Chang-hai, Dang Yuan-Yuan, and Zhao Jian-jun, "Hydraulic control on safety operation of large size flood-discharge tunnel under super-velocity flow," *Journal of Water Resources and Hydropower Engineering*, vol. 39, no. 4, pp. 94-97, 2008.

[13] S Mulligan and J Casserly, "The Hydraulic Design and Optimization of a Free Water Vortex for the Purpose of Power Extraction," Sligo, 2010.

[14] Omar B Yaakob, A H Elbatran, and M Ahmed Yasser, "CFD Validation for Efficient Gravitational Vortex Pool System," *Jurnal Teknologi (Sciences & Engineering)*, vol. 74, no. 5, pp. 97-100, 2015.

[15] (2015, September) Institute of Ecological Technology. [Online]. http://www.iet-community.org/research/research.html

[16] (2010, March) Focus on Micro Hydropower Projects. [Online]. http://dawn.com/news/967770/focus-on-micro-hydropower-projects

[17] CHEN Hong-xun, MA Zheng, ZHOU Yi LI Hai-feng, "Experimental And Numerical Investigation Of Free Surface Vortex," *Journal of Hydrodynamics*, vol. 20, no. 4, pp. 485-491, 2008.

[18] CHEN Hong-xun, MA Zheng, ZHOU Yi LI Hai-feng, "Formation And Influencing Factors Of Free Surface Vortex In A Barrel With A Central Orifice At Bottom," *Journal of Hydrodynamics*, vol. 21, no. 2, pp. 238-244, 2009.

[19] (2014, December) Living Water-Viktor Schauberger. [Online]. https://archive.org/stream/fa_Living_Water-Viktor_Schauberger/Living_Water-

Viktor_Schauberger_djvu.txt

[20] Sagar Dhakal, Ashesh Babu Timilsina, Dinesh Fuyal, and Nagendra Amatya, "Mathematical modeling, design optimization and experimental verification of conical basin: Gravitational water vortex power plant," in *World's Largest Hydro Conference*, Portland, 2015.

[21] Anjali Mohanan, "Power Generation with Simultaneous Aeration using a Gravity Vortex Turbine," *International Journal of Scientific & Engineering Research*, vol. 7, no. 2, February 2016.

[22] Christine Lepisto. (2007, June) Tree Hugger, Gravitational Vortex Power Plant is Safe for Fish. [Online]. http://www.treehugger.com/renewable-energy/gravitational-vortex-power-plant-is-safe-for-fish.html

[23] Zotlöterer turbine. [Online]. http://www.zotloeterer.com/welcome/gravitation-water-vortex-power-plants/zotloeterer-turbine/

[24] M J Khan, M T Iqbal, and J E Quaicoe, "River current energy conversion systems: progress, prospects and challenges," *Renewable and Sustainable Energy Reviews*, vol. 12, pp. 2177-2193, 2008.

[25] Sagar Dhakal et al., "Effect of Dominant Parameters for Conical Basin: Gravitational Water Vortex Power Plant," in *Proceedings of IOE Graduate Conference*, 2014.

[26] M Ahmad Yasser, H M Shabara, O B Yaaqob, and A H Elbatran, "CFD Simulation of Water Gravitation Vortex Pool Flow for Mini Hydropower Plants," *Jurnal Teknologi (Sciences & Engineering)*, vol. 74, no. 5, pp. 77–81, 2015.

[27] O Kiviniemi and G Makusa, "A Scale Model Investigation of Free Surface Vortex with Particle Tracking Velocimetry," 2009.

[28] A J Odgaard, "Free-surface air core vortex," *Journal of Hydraulic Engineering*, vol. 112, no. 7, pp. 610-620, 1986.

[29] R Gupta et al., "Studies on the understanding mechanism of air core and vortex formation in a hydrocyclone," *Chemical Engineering Journal*, vol. 144, pp. 153-166, 2008.

[30] J B Calven. (2003, March) The Vortex, Unviersity of Denver. [Online]. http://mysite.du.edu/~jcalvert/tech/fluids/vortex.html

[31] Tze Cheng Kueh, Shiao Lin Beh, Dirk Rilling, and Yongson Ooi, "Numerical Analysis of Water Vortex Formation for the Water Vortex Power Plant," *International Journal of Innovation, Management and Technology*, vol. 5, no. 2, April 2014.

[32] Ying-kui Wang, Chun-bo Jiang, and Dong-fang Liang, "Investigation of air-core vortex at hydraulic intakes," in *9th International Conference on Hydrodynamics*, Shanghai, China, 2010.

[33] Chen Yun-Liang, Wu Chao, and Wu Xiao-ming, "Hydraulic Characteristics Of Vertical Vortex At Hydraulic Intakes," *Journal of Hydrodynamics*, vol. 19, no. 2, pp. 143-149, 2007.

[34] Aurelien Davailles, Eric Climent, and Florent Bourgeois, "Fundamental understanding of swirling flow pattern in hydrocyclones," *Separation and Purification Technology*, vol. 92, pp. 152-160, May 2012.

[35] LI Hai-feng, CHEN Hong-xun, MA Zheng, and ZHOU Yi, "Experimental And Numerical Investigation Of Free Surface Vortex," *Journal of Hydrodynamics*, vol. 20, no. 4, pp. 485-491, 2008.

[36] Anotai Suksangpanomrung, Andrzej F. Nowakowski Wanwilai Kraipech Evans, "The simulation of the flow within a hydrocyclone operating with an air core and with an inserted metal rod," *Chemical Engineering Journal*, vol. 143, pp. 51-61, 2008.

[37] Punit Singh and Franz Nestmann, "Experimental Optimization of a free vortex propeller runner for micro hydro application," *Experimental Thermal and Fluid Science*, vol. 33, pp. 991-1002, 2009.

[38] Punit Singh and Franz Nestmann, "Experimental investigation of the influence of blade height and blade number on the performance of low head axial flow turbines," *Renewable Energy*, vol. 36, pp. 272-281, 2011.

[39] Sagar Dhakal, Ashesh Babu Timilsina, Dinesh Fuyal, and Tri Ratna Bajracharya, "Comparison of Cylindrical and Conical Basins with Optimum Position of Runner," *Renewable and Sustainable Energy Reviews*, vol. 48, pp. 662–669, 2015.

[40] S Wanchat and R Suntivarakorn, "Preliminary Design of Vortex Pool for Electrical Generation," *Journal of Computational and Theoretical Nanoscience*, vol. 13, no. 1, pp. 173–177, January 2011.

[41] S Wanchat, Ratchaphon Suntivarakorn, Sujin Wanchat, Tonmit Kitipong, and Pongpun Kayaniem, "A Parametric Study of Gravitational Water Vortex Power Plant," *Advance Materials Research*, vol. 805-806, pp. 811-817, 2013.

[42] Dhakal Subhash, Susan Nakarmi, Pikam Pun, and Arun Bikram Thapa, "Development and testing of Runner and Conical Basin for Gravitational Water Vortex Pool," *Journal of The Institute of Engineering*, vol. 10, no. 1, pp. 140-148.

[43] Christine Power, Aonghus McNabola, and Paul Coughlan, "A Parametric Experimental Investigation of the Operating Conditions of Gravitational Vortex Hydropower," *Journal of Clean Energy Technologies*, vol. 4, no. 2, 2015.

[44] Riccardo Ferreira. (2015, May) CFD Online. [Online]. http://www.cfd-online.com/Forums/main/75554-use-k-epsilon-k-omega-models.html

[45] Autodesk. (2015, May) Autodesk Help. [Online]. http://help.autodesk.com/cloudhelp/2014/ITA/SimCFD/files/GUID-E9E8ACA1-8D49-4A49-8A35-52DB1A2C3E5F.htm

[46] *ANSYS CFX-Solver Modeling Guide, Release 15.0.*: Ansys Inc., 2015.

[47] Chao WU, Bo WANGa, Min DU Yunliang CHEN, "Three-dimensional

Numerical Simulation of Vertical Vortex at Hydraulic Intake," *Elsevier*, vol. 28, pp. 55-60, 2012.

[48] S R Shah, S V Jain, and R N Patel, "CFD for Centrifugals: a review of the state-of-the-art," *Procedia Engineering*, vol. 51, pp. 715-720, 2013.

[49] S Mulligan and P Hull, "Design and Optimization of a Water Vortex Gravitational Pool," 2011.